69-16,661

NOBLE, Clyde S., 1933-
INVESTIGATION OF THE INERT GAS CONTENT OF HAWAIIAN INCLUSIONS THAT EXHIBIT ANOMALOUS AGES.

University of Hawaii, Ph.D., 1969
Chemistry, general

University Microfilms, Inc., Ann Arbor, Michigan

INVESTIGATION OF THE INERT GAS CONTENT OF HAWAIIAN INCLUSIONS THAT EXHIBIT ANOMALOUS AGES

A THESIS SUBMITTED TO THE GRADUATE DIVISION OF THE UNIVERSITY OF HAWAII IN PARTIAL FULFILLMENT OF THE REQUIREMENTS FOR THE DEGREE OF DOCTOR OF PHILOSOPHY IN CHEMISTRY JANUARY 1969

By

Clyde S. Noble

Thesis Committee:

John J. Naughton, Chairman
George Andermann
Clair E. Folsome
Arthur T. Hubbard
Ralph Moberly, Jr.

Acknowledgments

I am sure that the list presented below will inadvertently omit some of those who assisted my research and studies at the University of Hawaii. While apologizing to those omitted, I wish to thank the following:

Dr. L. Moore, Dr. J. Finlayson, and Dr. J. Funkhouser, former graduate students, and Charles Yamashiro for their advice and aid.

David Taylor and Hatsuo Taira for their assistance in the X-ray and solid-state mass spectrometry work reported in this dissertation.

Judy Kimura for the last minute compilation of a computer program.

Lee Aguiar for his work on flame photometry, mineral separation, sample preparation, mopping floors, and anything else I asked him to do.

Debbie, Carol, and Laura Noble for a last minute mineral separation.

Karen Okimura for her persistence and skill in the typing of the manuscript.

My wife for forgoing new dresses and nights-out and for insulating me from household worries for three and one-half years.

ABSTRACT

INVESTIGATION OF THE INERT GAS CONTENT OF HAWAIIAN INCLUSIONS THAT EXHIBIT ANOMALOUS AGES

An investigation was made of the inert gas content of some mineral inclusions from volcanic rocks. Potassium-argon dating of these inclusions has shown that they contain radiogenic argon in excess of that predicted by geochronological methods. Inclusions from Hualalai (Hawaii), Salt Lake Crater (Oahu), dredged from the Puna Rift east of Kilauea (Hawaii), and from Bultfontein, Republic of South Africa were examined. Specimens investigated were dunite nodules and separated grains of olivine, mica, pyroxene, and feldspar.

Existing gas extraction and mass spectrographic equipment was modified to allow helium analysis, and also to make the entire gas analysis more rapid and convenient. A technique was developed for the analysis of potassium in olivine by flame photometry.

The results from this study indicate that a similarity exists in helium-to-argon ratios found in inclusions from different sources and that the absolute inert gas content varies significantly within individual samples. The excess argon found in the deep ocean tholeiite cautions against the use of similar samples for potassium-argon dating.

This study reaffirms the theory that the excess radiogenic argon found in some minerals is held in fluid inclusions and that these minerals do not yield consistent or significant ages.

Table of Contents

List of Tables

List of Figures

I. Introduction and Background

Early in the 19th century geologists in England and France[10,45] laid the groundwork for the new field of geochronology by identifying and correlating successive rock strata according to the fossils contained in each layer. This eventually evolved into a means of determining a relative age scale. Several attempts to establish an absolute age scale were subsequently made. Generally, these attempts were based on estimates of the rates of sediment deposition, denudation, or of organic evolution. These estimates were, as would be expected, rather subjective and resulted in a wide range of estimated ages. An article published by J. Barrell in 1917[6] affords some insight into the uncertain state of absolute geochronology at the time. For example, he presented a table containing the best age estimate of six contemporaneous workers. The estimates of ratios of the duration of consecutive periods varied by a factor often as large as 30 and the sums of the ages from Recent through the Cambrian period varied from 25 to 700 million years.

Shortly before this time the laws of radioactive decay had been discovered and it had become obvious that here was an essentially invariable phenomenon that could furnish the absolute time scale that geologists desired. Since then, several methods of absolute geochronology have evolved. Most of these methods are radiochemical in nature

and are based on the principle that a parent radioactive atom will decay to its daughter atom by a course that is observable in regard to both its rate and nature. The assumptions made in radioactive dating are: 1) the rate of decay of the nuclide is constant and is accurately known, 2) parent and daughter concentrations can be measured accurately, and 3) the system has remained closed in regard to parent and daughter since the geological event under consideration. The second assumption can be qualified in that what is actually required for calculation of a radio-age is the concentration of either the parent or daughter and the number of decays occurring since the geological event. In most cases this is satisfied by measuring the concentration of both the parent and daughter, however, this is not necessary if, as in the case of fission-track dating, the number of radioactive events can be counted directly. The existence of a closed system is often open to question but experience and experimentation has shown what minerals may best be utilized and under what circumstances these minerals may be expected to yield true ages. Table I was compiled to summarize the basis and the limitations of some of these methods. It can be seen that one of the most widely applicable methods is that using the potassium-argon couple. The uranium-helium method could be almost as useful a technique were more known about helium retention in uranium minerals. Both techniques involve rare-gas analysis.

Table I

Principle Radiodating Techniques

Radiodating Technique	Useful Range: my	Utility of Technique	References
^{40}K-^{40}A	>0.1	Wide applicability due to ubiquitous occurrence of potassium and favorable half-life.	2,3, 26,32
^{87}Rb-^{87}Sr	>10	Rubidium is not abundant but is widely distributed. Half-life is based on geochronology.	1,9, 26
^{232}Th-^{208}Pb	>10	Lead isotopic analysis can be difficult but since uranium and thorium usually occur together, four independent calculations can be made. Thorium and uranium are not abundant.	8,19, 26
^{235}U-^{207}Pb	>10	Restricted to uncommon ore bearing rocks.	8,19, 26
^{238}U-^{206}Pb	>10	Less sensitive to original lead correction but hexavalent uranium can be readily leached.	8,19, 26
^{207}Pb-^{206}Pb	>500	Technique is complex and sensitive to errors in original lead correction.	8,19, 26
^{14}C	<0.07	Generally applicable only to young carbonates. Assumes no variation in atmospheric ^{14}C level.	26,39

Table I (Cont.)

Principle Radiodating Techniques

Radiodating Technique	Useful Range: my	Utility of Technique	References
U,Th-He	$>10^{a}$	Suffers from easy loss of helium. Technique is not well received at present.	2,12, 26
^{187}Rh-^{187}Os	a	Molybdenite is the only mineral with a sufficient rhenium content. Half-life based on geochronology.	26,29
^{176}Lu-^{176}Hf	a	Lutetium is very rare.	34
Fission track	$>10^{-4}$	Limitations imposed by uranium content but the technique holds promise, although still in development stage.	21,52
Radiation Damage	a	Little conclusive work done. Damage is also a function of thermal history.	18,30
Ionium	>0.3	Use has been limited to marine sediments and corals.	33,59

a - A useful range is difficult to assign due to limited work done on these techniques or due to lack of knowledge of daughter retention by the minerals.

The history of the development of the potassium-argon and the uranium-helium techniques has been ably reviewed by several authors[32,34,22] and need not be repeated here. It should suffice to say, however, that only recently have these techniques been reduced to a fairly reliable practice. The potassium-argon method, in particular, has been applied to increasingly difficult problems and has led investigators into areas, such as gas diffusion in minerals and ultra-trace analysis, that may seem somewhat removed from geochronology. These complimentary investigations usually arise when a geochronological method is pushed to its ultimate sensitivity and when anomalies are still evident. The importance of these auxiliary investigations lies in their ability to explain the anomalies, define the analytical limits of existing methods, and to suggest new directions for geochronology research. It is in these ancillary areas that the problem of accuracy and sensitivity become acute. The solution of some of these problems which relate specifically to inert gas geochemistry may have significance beyond the dating technique along and extend into questions concerning the chemistry and origin of the earth, of meteorites, and of the solar system. It is the study of one of these areas, that is, the very old ages obtained for certain volcanic rocks, which forms the basis for work reported here.

When "too young" ages are obtained the anomalous results are usually attributed to diffusional or leaching

losses of the daughter isotope of the measured pair, although if additional parent isotope were acquired by the mineral the result would be the same. If the parent were lost or the daughter acquired "too old" ages would result. In the case of the potassium-argon ages the anomalous old ages are explained as being due to inherited inert gas, since a natural process that would remove the parent potassium would probably do so by opening the lattice and then the associated argon would also be lost. Among rocks exhibiting anomalous old ages are the olivine inclusions as described by Naughton[23] and others.[55] The term "inclusion" will be used throughout this dissertation to refer to a fragment of a mineral that is included or contained in another mineral or a rock. The dunite nodules found at Hualalai will be considered a special case of an inclusion since the mineral is not included in the host basalt. The nodule, in this case, became separated from the basalt shortly after eruption and before the lava had a chance to solidify and include the nodule.

A gaseous or liquid inclusion within a mineral grain will be referred to as a fluid inclusion.

Olivine inclusions are found at sites scattered throughout the world. Roedder,[55] in his study of fluid inclusions, lists examples from New Zealand, South Africa, Europe, North America, and Hawaii. The inclusions can be found in basaltic rock, as at Salt Lake Crater, Oahu, Hawaii

or as discrete dunite nodules as in the 1801 Kaupulehu flow at Hualalai, Hawaii. Three hypothesis generally proposed for the origin of inclusions are that they represent either, 1) xenolithic fragments of rocks existing in the crust or upper mantle that have been broken away from the conduit walls and transported to the surface in the magma, 2) xenolithic fragments of the residue from a partial or total fusion of the fusible portion of the primary mantle material, or 3) segregations of denser materials that were crystallized within the magma.

Ages of up to 8 billion years have been reported using the potassium-argon and the uranium-helium methods for dunites and peridotites, respectively. It has been tentatively established by Naughton and co-workers[22,23] that this inherited inert gas, in the case of argon at least, is contained in the fluid inclusions found in practically all minerals.[25] Fluid inclusions is here meant to include both gaseous and liquid inclusions.

The similarity of the mineral inclusions from widely scattered areas has suggested, to some workers, a similar origin. The chemical and petrological aspects of many of these inclusions have been investigated by Jackson,[36] by Green,[24] and by White.[61] Jackson concluded that a relation probably exists between the growth of Hawaiian volcanoes and some mineral inclusions, and that these inclusions may be formed in the crust. Green examined the Salt

Lake "eclogites" in the light of recent experimental studies of melting and subsolidus relations in basaltic rocks at high pressure, and concluded that these eclogites (garnet-pyroxenite) are not examples of primitive magma or of the mantle. White's comprehensive petrological and electron microprobe study of a number of ultramafic Hawaiian inclusions led him to conclude that these inclusions are separable into three suites which correlate with types of basaltic hosts. The differences observed among these suites suggests more than one origin for the inclusions. He suggests that the olivine tholeiite inclusions formed within the enclosing magma, and that the lherzolite inclusions found in olivine nephelinite, nepheline basanite, and ankaratrite may have originated in the mantle. He points out, however, that these inclusions may or may not be representative of the mantle since they may be the infusible residue of the mantle. He also advises that a large body of refined descriptive data will be needed before general agreement can be reached as to the probable origins of these inclusions.

This study was undertaken with the thought that a more thorough investigation of the inert gas content of some of these inclusions might be able to supply answers to some of the following questions:

1. Are the inclusions xenolithic or segregative in origin?

2. Is the inert gas content of these inclusions that which would be expected to arise from the decay of naturally occurring radioactive potassium and uranium?
3. Can meaningful ages be determined on these inclusions by means of normal inert gas geochronological methods?
4. Are the inert gases formed within the inclusions, or are they incorporated into the inclusions from the magma environment?

The inclusions have been studied for over a century and their origin is still controversial. Since various features of the inclusions are used to support assorted hypotheses relating to the origin of basaltic magma or the nature of the mantle or crust it can be seen that the answers to the above questions are important not only to geochronology but also to petrology and the study of the crust and magma.

II. Experimental

The research described here is, in part, an attempt to extend radiochemical geochronological studies to ultrabasic rocks containing a very low concentration of the radioactive elements and their decay products.

The experimental work necessary for this involved the following steps: 1) sample selection and preparation, 2) study of extraction techniques and application of these techniques to ultramafic inclusions, 3) study of mass spectrometric procedures in regard to optimizing sensitivity and reproducibility for the determination of the argon isotopes and helium, and 4) development of a sensitive method for low level potassium analysis.

In the description of the apparatus and of the operating procedures that follows it is desirable to treat these matters at some length. Mass spectrometry and high vacuum techniques border on the occult and it is felt that a detailed description may be helpful for the guidance of future work.

A. Equipment

1. Gas Extraction and Purification System

Gas extraction was accomplished by either melting or grinding the rock samples. The purification of the gases released was achieved by selective adsorption on "molecular sieve" zeolites and chemical gettering by titanium and by copper-oxide. The extraction and purification system is presented schematically in Figure 1. The areas enclosed by

dashed lines represent the sections that were baked out periodically.

Several modifications have been made since the system was constructed by Funkhouser.[22] In the originally designed system the extracted gas samples were isolated and removed from the extraction unit in small break-seal ampoules. The ampoules were then added to the sample section (D, Figure 1) for analysis. In the apparatus used for this study, the extraction unit was connected directly, through valve #6 (Figure 1) to the mass spectrometer system. This was done for two reasons; 1) to minimize chances for contamination and loss of sample through the mishandling of break-seal sample ampoules, and 2) to enable analysis of helium to be carried out. Since helium cannot be condensed on charcoal at liquid nitrogen temperatures along with argon, it occupies the entire extraction system and a recovery of about 0.2% resulted when the sample was collected in the break-seal ampoule. This is a consequence of the fact that the volume of the ampoule was about 3 cm^3 and the volume of the extraction system was about 1500 cm^3. Because this step was eliminated, the recovery was increased to about 20% and was reproducible in the arrangement used in this work. If, upon expansion of the sample into the mass spectrometer, the total gas pressure was too high, attenuation of the ion beam resulted in a loss of sensitivity. With the present arrangement, the sample could be moved back into the gettering

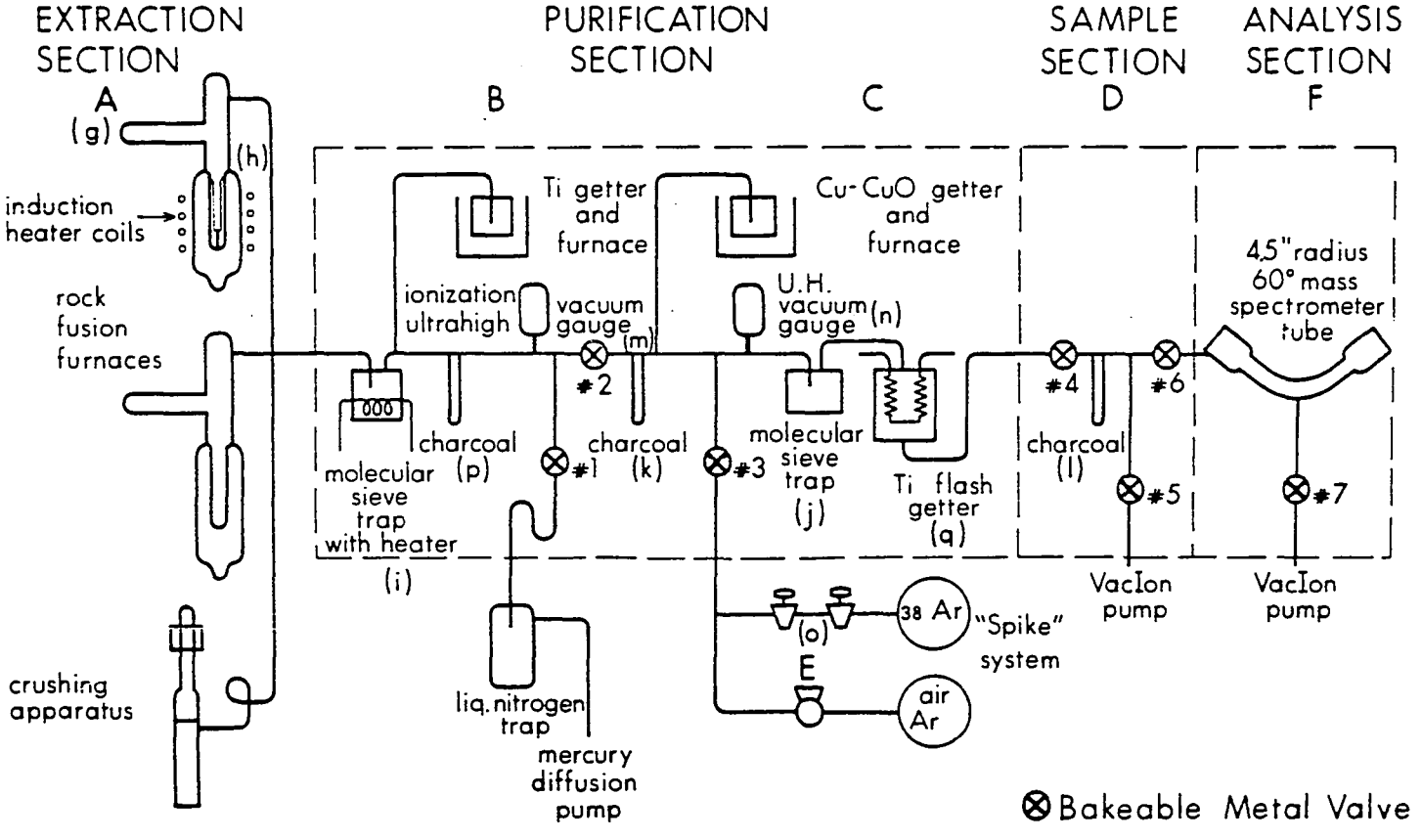

Figure 1

Schematic Diagram of Inert Gas Extraction, Purification, and Analysis Apparatus

system for further purification, or a fraction of the sample discarded by manipulation of the various valves of the extraction system.

The reactors (A, Figure 1) were constructed of quartz, rather than pyrex, since higher temperatures and more severe temperature gradients would be encountered during the fusion of the high melting olivine than would be met in work on normal rocks. The design of the crucibles and the reactors was such that more than one sample could be run in each molybdenum crucible. The procedure used by Funkhouser[22] and some other workers[12] involved opening the extraction system after each determination. This in turn necessitated a bake-out of the system after each determination and thus required a substantial amount of glassblowing. By placing a side arm on the reactor (g, Figure 1) and supporting the crucible from below, it was possible to separately pretreat the mineral samples in the side arm and to degas the crucible with the induction heater and then, by manipulating an iron push bar by means of a small magnet, cause the sample to fall into the crucible for melting. In this way two or three samples could be melted in one crucible. Since each of the two reactors could be used for three samples, the number of times the system had to be opened to the atmosphere and baked out was reduced by a factor of six. As a result, the consumption of crucible metal, bakeable valves, and oven heating elements was greatly reduced, and a reduction of operating time and cost was realized.

The crucibles were constructed out of 0.018 cm or 0.015 cm thick molybdenum sheet. It was found that a crucible made of 0.018 cm thick molybdenum sheet was necessary when melting the olivine samples because the thicker metal better withstood the repeated high temperature treatment. The crucible consisted of a cup that was pressed out of a single circular piece of molybdenum sheet and was 2.0 cm in diameter and approximately 0.6 cm deep. A collar 9.3 cm in height fitted into the cup and was flared at the top to fit snugly into the neck of the reactor (h, Figure 1). Extended experimentation with combinations of crucible wall thickness and various induction coil sizes was necessary to establish the conditions under which more than one olivine sample could be fused in each crucible without the crucible deteriorating to the point where it could no longer be heated to a temperature sufficient to melt additional samples.

A radio frequency induction heater of 5 KW power was used (Model T-5-3-KC-L-S, Lepel High Frequency Laboratories, New York, New York) which enabled temperatures of at least 1800°C to be obtained when using a coil of 5.1 cm i.d. with approximately one turn per cm. This is the approximate melting point for olivine and was verified by measurements with an optical pyrometer. (Leeds and Northrup, Philadelphia, Penna.)

The titanium getter section (B, Figure 1) was isolated by valve #2 from the copper-copper oxide getter section

(C, Figure 1) to reduce the gettering load on the copper-copper oxide getter.

The tracer addition system (E, Figure 1) utilized in these experiments was a pipette type rather than the more common break-seal type. In the break-seal system used by Funkhouser the tracer was isolated in a break-seal ampoule (~3 cm^3 volume) at a known pressure. The ampoule was then attached to the extraction system by glass blowing and the tracer introduced by breaking the break-seal with a small iron bar and magnet. The pipette system employed in this work was similar to that used by Dalrymple[11] but was used here to introduce the tracer directly into the system rather than to prepare break-seal tracer ampoules ("spikes"). This will be discussed in greater detail in section 3.

A similar pipette system (E, Figure 1) was used to introduce air argon samples into the system.

Molecular sieve traps of the types described by Biondi[7], containing 15 to 25 g of Linde molecular sieve 13A, were placed in both sections of the extraction and purification system (i and j, Figure 1). The trap in section B was fitted with an internal nichrome wire heating element that enabled the trap to be degassed at an elevated temperature between determinations. Each section also had a quartz cold finger (p, k, and l, Figure 1) containing 0.5 to 1 g of activated wood charcoal.

The titanium getter consisted of a 6.4 cm o.d. by 10.2 cm high stainless steel can containing approximately

25 g of titanium sponge. The can was heli-arc welded and fitted with a graded seal joining the Kovar metal to glass tubing. The stainless steel to Kovar seal was accomplished using a high temperature silver solder. The getter was heated with a nichrome wire resistance furnace and the temperature measured with a chrome-alumel thermocouple.

The Cu-CuO getter (C, Figure 1) consisted of 50 to 100 g of 20 mesh copper oxide rolled up in a copper screen plus 1 to 2 g of silver moss in a stainless steel can similar to that described above for the titanium getter. A similar resistance furnace was used to heat the getter and the temperature was measured with a mercury thermometer.

Each section also contained Bayard-Alpert ionization gauges (m and n, Figure 1) for measuring the pressure in the respective sections. A single read-out and control unit was available so a plug-in arrangement was constructed to make switching from one gauge to the other more convenient.

A crushing apparatus of the design utilized by Funkhouser was used in the crushing experiments (Figure 2). The dimensions of the stainless steel mortar were approximately 2.5 cm o.d. and 10.2 cm high. The pestle was also stainless steel and was 0.6 cm o.d. and 0.18 cm high and was fitted with a stainless steel rod with a small iron armature at one end. The armature fit snugly into the 1.0 cm glass tubing at the top of the mortar. A small electromagnet fit over the glass tubing and was intermittently activated to

lift the pestle and cause it to fall on the rock sample. A microswitch was used to turn the current to the electromagnet on and off. The microswitch was in turn activated by an eccentric cam that rotated at a speed that resulted in the pestle rising and falling about 70 times per minute.

A titanium flash getter (q, Figure 1) was used for final gettering when necessary. This getter consisted of a tungsten filament wrapped with titanium and tantalum wire sealed in a glass envelope. When the tungsten wire was heated by passing current through it, the titanium and tantalum were vaporized and formed a highly active gettering surface upon condensing on the glass envelope walls.

The entire purification section could be baked at 400°C with an oven constructed with walls of Maranite (compounded magnesite board, Johns Mansville and Co.) and utilizing four quartz I.R. lamps (G.E., type 500T3) for heating. The samples, reactors, and crusher were heated separately with a combination of small tube furnaces, small resistance ovens, and heating tapes.

2. Sample Section

The sample section (D, Figure 1) consisted of a titanium getterion pump (Vac-Ion pump, 8 L/sec., Varian Associates), a quartz charcoal cold finger (1, Figure 1) and appropriate valving (see Figure 1). This section was retained for two reasons: 1) To provide an isolated section for attaching samples from a second extraction system, and

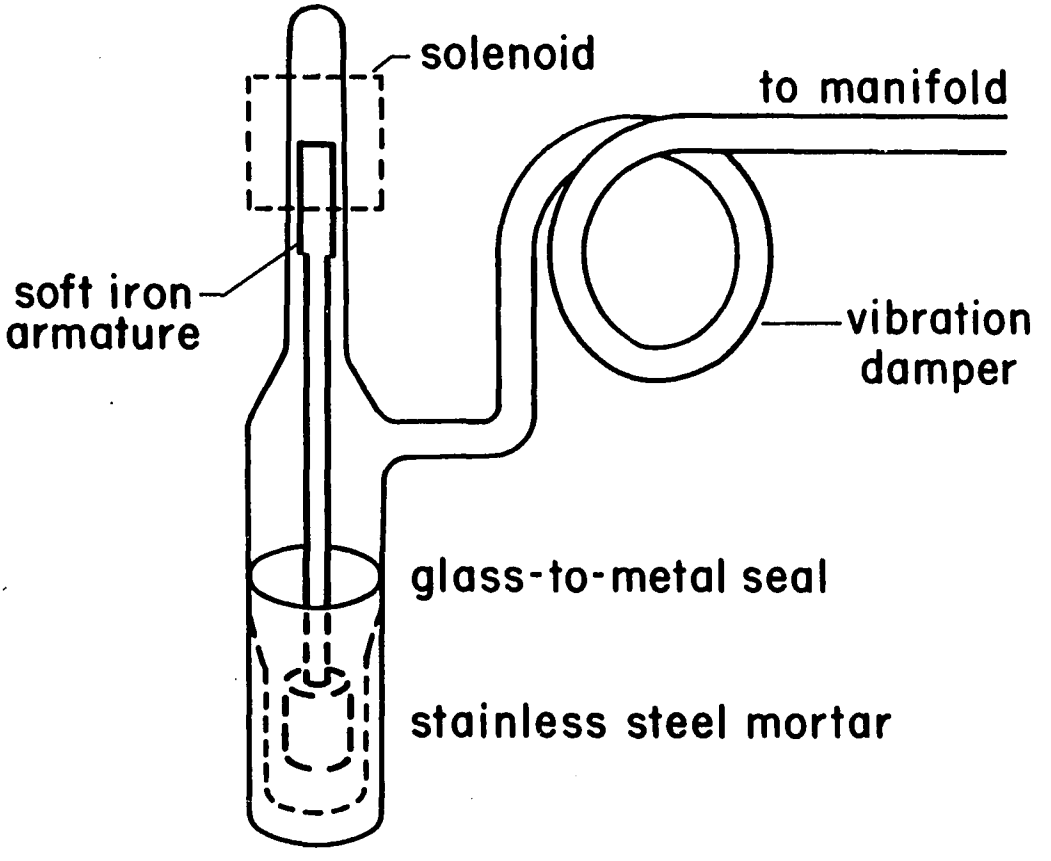

Figure 2

Crushing Apparatus

2) To provide a small volume reservoir so that maximum sensitivity could be achieved upon expansion of the sample into the mass spectrometer. It was constructed so that it also could be baked out.

3. Argon-38 Tracer Addition Section

The tracer addition system is shown at E in Figure 1. The two stopcocks were of a hollow-barreled, hand-lapped type, lubricated with a mixture of Apiezon "N" (James G. Biddle Co., Plymouth Meeting, Penna.) and molybdenum sulfide. The pipette volume for the argon-38 system was 2.41 cm^3 and the argon-38 reservoir was a 1 L bulb with an initial pressure of argon of about 3×10^{-4} torr. The argon-38 used to prepare the argon-38 reservoir was obtained as a 0.1 std cm^3 sample from the Institute of Physical Chemistry, University of Zurich, Switzerland, and was of 99.98% isotopic purity.

The tracer addition technique was in most laboratories using the isotope dilution technique for mass spectrometric argon analysis utilized small ($\sim$ 3 cm) break-seal ampoules containing a known amount of argon-38. These ampoules were prepared on a separate vacuum system in which a McLeod gauge was used to measure the pressure of the gas in the system. The volume of each ampoule was carefully determined and hence the absolute amount of argon-38 present in each ampoule could be estimated. However, a great deal of care must be taken at each step to obtain consistent and accurate estimations, i.e., in obtaining a clean system with a known pressure,

in removing the ampoule with a predetermined volume from the preparation system, and in adding the ampoule to the mass spectrometer system. As a result, frequent calibrations must be made and any one tracer is still subject to a certain doubt as to its validity. Dalrymple[11] described a pipette system used to prepare tracer ampoules in place of the usual volume dilation technique. It was decided to attempt to use a modification of this system to introduce the tracer directly into the extraction system. This would avoid much of the glass blowing chores and also would provide greater versatility in that it would be possible to introduce one or more tracer volumes as needed to check the sensitivity of the mass spectrometer at almost any time, and also to add the tracer at any stage during the run. It was felt that this technique afforded the best compromise between accuracy and practicality available at the time. The main disadvantage of this system was that the argon-40 and helium level in the tracer showed a slow but definite increase with time. It was believed that most of the contamination resulted from diffusion of these gases from the air through the grease used to lubricate the pipette stopcocks. If an all-metal pipette of the types described by Heymann and Keur[28] could be used, this difficulty could largely be eliminated. Figure 3 shows a calibration curve obtained using the United States Geological Survey (U.S.G.S.) muscovite P-207[38] as a standard. The relative standard deviation for this set of

tracers was 1.3%, which is comparable to the precision achieved with other techniques.[11]

4. Air Argon Pipette System

A reservoir bulb and a glass pipette system was attached to the extraction system at the same place as the argon-38 tracer system (E, Figure 1). The pipette for the air argon was a single 4-way, hollow-barreled stopcock with a glass tubing loop ($\sim$2 cm^3 volume) for isolating the aliquot of air argon. The air argon reservoir was prepared from a reagent grade bulb of argon obtained from Air Reduction Co. The argon-40 to argon-36 ratios measured on these samples were used to calculate the amount of argon-40 present in the gas samples due to atmospheric argon contamination. Several break-seal ampoules of dry air at a low pressure were prepared and analyzed for the natural argon-40 to argon-36 ratio. The ratios measured for these samples agreed well with those from the pipette system.

5. Mass Spectrometer

The mass spectrometer used in this study was a 4.5 in., 60° sector, single focusing glass enclosed instrument of the type originally designed by J. H. Reynolds.[54] The mass spectrometer tube was purchased from Nuclide Corp., State College, Penna. and the accessary components were either constructed or purchased.

A schematic drawing of the spectrometer is shown at F in Figure 1. There were two openings to the mass spectrometer.

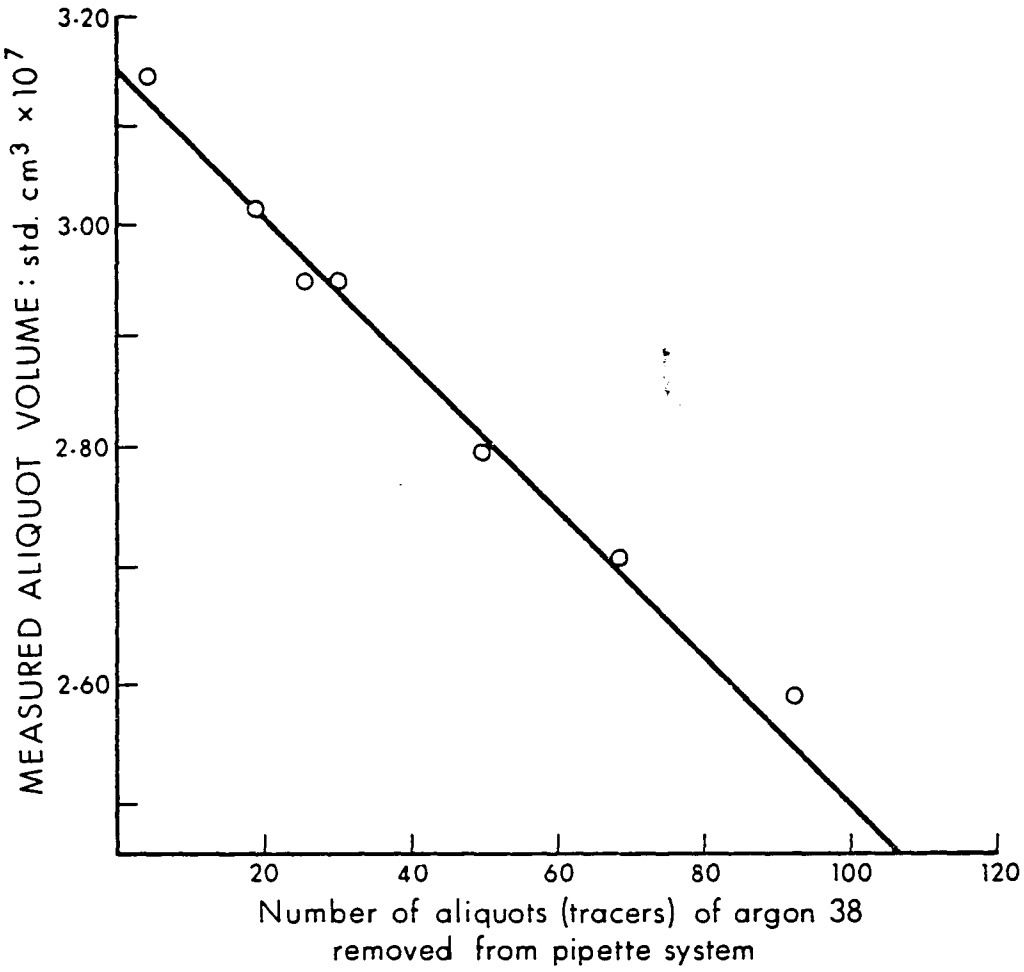

Figure 3

Analysis of Interlaboratory Argon-40 Standard

One was the sampling inlet through valve #6 (Figure 1) and consisted of a 0.4 cm glass tube leading directly into the ion source from the sample section. The other was an outlet to the titanium getter ion pump through valve #7 (Figure 1). The tube was made of pyrex glass and was supported in a horizontal position by three Maranite blocks. Both ports were fitted with all-metal bakeable valves. The filament emission regulator was designed for use with another type of mass spectrometer and had to be modified for use with the larger filament used in this ion source. Accelerating and focusing potentials were maintained by a voltage divider fed from a 2 KV dc power supply. (Model 412B, John Fluke and Co.) The mass range was scanned by varying the current in the electromagnet. A magnet current of about 110 mA provided a field of approximately 3.78 kilogauss which focused ions with a mass-to-charge ration of 40 at the ion collector. A magnet current of about 250 mA was attainable. The current could be varied either manually or electronically. The regulator, its supply, and the magnet were all purchased from the Nuclide Corp. The field strength was monitored with a Hall Effect indium-arsenide probe and a RFL Gaussmeter. (Radio Frequency Laboratories, Boonton, New Jersey)

The ion current was measured with a Faraday cage and a Cary model 31 vibrating reed electrometer. (Applied Physics Corp., Monrovia, Calif.) The collector was shielded with a graphite coating on the glass parts and with a steel box

over the entire assembly. A 1 to 100 mv Leeds and Northrup recorder with a 7-inch chart was used to record output from the electrometer. The filament emission regulator, dc power supply, magnet power supply, and electrometer were all supplied from a constant voltage transformer in order to minimize signal variations due to line voltage fluctuations.

The operating parameters used for optimum argon sensitivity were arrived at experimentally and differ only slightly from those used by Funkhouser[22] for this instrument. They are listed below:

Trap current	26 microamps
Filament current	3.9 amps
Case voltage	48 volts
Case current	1.0 milliamps
Trap current	147 volts

A complex relationship existed between these parameters and the ion current. The magnet current also affected the source characteristics, probably as a result of the fringe magnetic field. The small discrimination observed with this instrument probably arose as a result of the changing fringe field acting upon the ion source. Under these conditions an overall sensitivity of approximately 1×10^{-9} std cm^3 per mv for the argon isotopes was obtained. The output noise level of approximately 0.2 mv resulted in a lower level of detection of about 2×10^{-10} std cm^3 of argon. (For a signal-to-noise ratio of 1:1) It will be shown later, however, that the overall sensitivity includes factors other than the detector sensitivity.

The residual gases in the mass spectrometer consisted of ions with mass-to-charge ratios (mass numbers) of 1,2,16, 17,18,28,32, and 44. The relative peak heights varied with time and conditions, but the 28 peak usually was the largest. A mass 35 peak was not usually observed, although it was reported by Funkhouser[22] that this instrument had residual mass 35 and 37 peaks. The operating procedure had been changed so that the filament current was left on continuously. This apparently was responsible for the reduction in background that has been observed. When the mass spectrometer was isolated from its pump, a memory effect for the argon isotopes and for helium could be observed. The rate of increase of the mass peaks varied from one time to another, probably as a result of the slow release from the spectrometer components of gases adsorbed during the recent history of the system. The rate of increase for the isotopes of interest was approximately as follows: Mass 36- negligible, 38- 1.5×10^{-9} cm^3 sec^{-1}, 40- 8×10^{-9} cm^3 sec^{-1}, 4- 5×10^{-9} cm^3 sec^{-1}.

6. Flame Photometer

The flame photometer used for this study was a filter flame photometer (Model 143, Instrumentation Laboratory, Inc., Watertown, Mass.) that used three optical filters and photocells for measuring the sodium, potassium, and lithium radiation from a propane-air flame. The sample was aspirated into an atomizer chamber where part of the sample was carried

into the flame by the air feeding the flame. The air was supplied by an oilless compressor (Bell and Gossett Div. of IT&T) and filtered. This arrangement minimized the effect of contaminates in the air since the air in the spray chamber was supplied by the compressor and filtered prior to entering the spray chamber. The instrument was designed for use with the lithium internal standard technique exclusively. There were three read-outs, two digital for sodium and potassium and an emission level indicator for lithium. The instrument had zero and balance controls for the sodium and potassium read-outs and a lithium-set control for calibration. The instrument could be calibrated so that the minimum potassium response (one unit) corresponded to 0.01 ppm potassium. Under proper conditions, the reproducibility of successive measurements was at least ±0.02 ppm potassium for dilute solutions.

If the solution being analyzed contained high concentrations of interfering ions the radiation from all three analyte elements was often greatly reduced. If the output from the lithium detector fell below a pre-set level, the output from the sodium and potassium detectors was no longer displayed at the digital read-out and it was then necessary to reset the lithium emission indicator manually. A direct read-out of the potassium concentration was no longer possible, unless the instrument was recalibrated using standards containing the same interfering ions at similar concentrations.

B. Sample Selection and Preparation

The rock specimens used in this study and the methods of sample preparation are described in Table II. The specimens were collected by several different workers from the locations indicated in Table II.

In some cases whole rock samples were used for determination and in some cases the various minerals were separated before the samples were taken for determinations. In the case of the dunites it was believed that the whole rock was of interest so in most cases mineral separation was not carried out. In some instances, intact sample sections as large as could be handled conveniently were used in order to minimize possible losses of included inert gases during grinding.

C. Gas Extraction and Determination Procedure

The procedure for the inert gas extraction and determination may be summarized as follows:

1. Samples and crucibles were sealed into the system.
2. Samples and extraction and purification systems were baked out and the entire system was tested for leaks.
3. A known amount of argon-38 was introduced into the extraction system.
4. Gases were extracted by melting or crushing the rock sample.
5. Inert gases were purified by chemical and sorption gettering.

Table II

Description of Specimens and Samples

Specimen Number	Description of Specimen	Method of Sample Preparation
HK-137	Olivine gabbro nodule about 15x15x15 cm from 1801 Kaupulehu flow, Hualalai, Hawaii. Consisted of olivine with p phenocrysts of feldspar and pyroxene.	A large section of the nodule was broken and a 32-60 mesh fraction separated magnetically into the three mineral fractions.
HK-160	Dunite nodule about 10x10x14 cm from same location as above.	Sections about 2x2x2 cm (Fig. 9) were cut from nodule and broken without grinding. Individual samples selected by quartering.
HK-161	Dunite nodule about 6x6x6 cm from same location as above.	Same as above.
HK-162	Deep ocean tholeiite dredged from east rift zone of Kilauea at depth of 4680 M. Very little alteration. Largely opaque glass with 15% olivine inclusions. Pieces ranged in size from 0.1 to 4 cm in diameter. Location #12, reference 49.	Interior, less glassy pieces used when possible. Some olivine separated by hand.
HK-166	Dunite nodule about 20x25x30 cm from same location as HK-137. Some chromite present.	Section about 1x1x5 cm cut from nodule and small, intact pieces used for determinations.

Table II (Cont.)

Description of Specimens and Samples

Specimen Number	Description of Specimen	Method of Sample Preparation
HK-167	Feldspar-pyroxene nodule from same location as HK-137.	Center and edge sections about 4x4x4 cm were cut from nodule, broken to 32-60 mesh and separated magnetically.
HK-168	Olivine nodule about 10x10x15 cm with olivine extensively altered to iddingsite.	A section from the nodule edge was broken to 32-60 mesh and the fractions separated magnetically.
HK-170	Composite of several small inclusions from north shore of Salt Lake, Oahu, 2 to 3 mm particles. Consisted of olivine and about 15% diopside.	Diopside and olivine were hand separated magnetically.
HK-172	Deep ocean tholeiite dredged from east rift zone of Kilauea at depth of 2590 M. Pieces ranged in size from 0.1 to 4 cm in diameter. Location 10, reference 49.	Interior, less glassy pieces used when possible.
HK-173	Same as above, from a depth of 1400 M. Location 4, reference 49.	Same as above.
HK-174	Olivine-pyroxene nodule from Bultfontein, Republic of South Africa, courtesy of Dr. Kalbe, Univ. of Capetown, R.S.A. Contained about 5% olivine, mostly pyroxene.	Sample crushed to 16-25 mesh and an attempt was made to separate the fractions magnetically. Olivine hand separated from olivine-rich fraction.

Table II (Cont.)

Description of Specimens and Samples

Specimen Number	Description of Specimen	Method of Sample Preparation
HK-175	Composite of several small kimberlite inclusions from the north shore of Salt Lake, Oahu.	Mica was hand separated and used without further treatment.
P-207	U.S.G.S. muscovite. Interlaboratory standard.	Used as received. Standard mixed thoroughly before each sampling.
R-1659	Zircon from Renfrew Co., Ontario, Canada.	Mineral mixed thoroughly before each sampling.

6. Helium and argon were analyzed by mass spectrometry.

These steps are discussed in detail below.

1. Sealing samples and crucibles into the system. The crucibles were assembled and degreased by washing with acetone. After the crucible had been carefully positioned in the reactor, the weighed samples, wrapped in aluminum foil, were placed in the reactor side arms. Platinum foil was used for samples such as the standard muscovite that might decrepitate severely enough during heating to be ejected from the crucible. A small iron bar was also placed in each side arm. The reactor was then glass-blown onto the system and tested for leaks with a Tesla coil.

2. Degassing the system. The bake-out oven was then placed over sections B and C (Figure 1) and heated at 400°C overnight. The titanium getter furnace was also turned on so that the getter temperature was about 840°C during the bake-out. The reactors, side arms, and crushing apparatus were all baked out at lower temperatures to reduce the possibility of argon losses from the samples and to lessen the strain on the various graded seals. The samples in the side arms were heated to about 200°C, the reactors to about 200°C, and the crusher morter to about 150°C. After the bake-out was completed and the system had cooled to room temperature the entire system was checked for possible leaks by closing the system to the pumps for five minutes and then measuring the pressure. If the pressure rose no higher than 3×10^{-6}

torr the system was considered leak-free and the determination started.

3. Introduction of argon-38 tracer. The argon-38 tracer was first isolated in the pipette (O, Figure 1) after allowing about five minutes for equilibration with the argon-38 reservoir. The tracer was drawn into the extraction part of the system by placing liquid nitrogen on the charcoal finger (b) in that section for one hour after opening the stopcock (o). Kirsten[37] has shown that one hour is necessary to complete such an operation. It was found that it was necessary to pump off the non-condensable gases, mainly helium, from the tracer system by opening valve #1 (Figure 1) for about 15 minutes while the liquid nitrogen was still on the charcoal cold-finger. No evidence of argon loss during this treatment could be found, either by direct observation of the height of the argon-38 peaks, or by comparison of results from standard samples analyzed using this technique with results from analyses carried out without removing the helium in this manner.

4. Extraction of Gases. After the tracer transfer was complete, the valve between the titanium getter section and Cu-CuO getter section (valve #2, Figure 1) was closed. The liquid nitrogen was left on the cold finger (p) and the titanium getter not heated during the sample fusion to keep the pressure as low as possible in order to avoid high pressure glow discharges in the reactor. The induction heating

was usually continued for a total of at least 6 minutes at a power setting that was known to produce a temperature sufficient to melt the sample. As soon as the induction heating was completed the titanium getter furnace was turned on.

In the crushing runs, the titanium getter furnace was turned on at the time the crusher was started. The crushing was continued for 4 hours and then the titanium getter furnace and the crusher were turned off.

5. Purification of gases. The titanium getter reached 800°C in approximately 1 hour and 20 minutes and was maintained at that temperature for at least 1 hour. The liquid nitrogen was left on the cold-finger after melting and valves #4 and #2 (Figure 1) were opened and valve #5 closed. About 30 minutes were allowed for equilibration of the gases and then valves #4 and #7 were closed and valve #6 opened, allowing the gases to expand into the mass spectrometer. The mass 4 and the mass 40 peaks were monitored and their "time zero" values determined. The mass 40 volume was usually less than 0.5×10^{-9} std cm^3. The operation of the mass spectrometer will be described in detail in a later section. When the titanium gettering was completed, the titanium getter furnace was turned off and allowed to cool to about 400°C before opening the valve between the two purification sections (valve #2). At this point most of the removal of reactive gases should be completed. The object in allowing

the titanium getter to cool before exposing the gases to the Cu-CuO getter was to allow most of the hydrogen present to be readsorbed by the titanium at 400°C, the temperature for maximum adsorption of hydrogen by titanium, and thus greatly reduce the extent of the hydrogen-CuO reaction. This would make the CuO more efficient in converting the small amount of carbon monoxide present to carbon dioxide. The carbon dioxide in turn would be adsorbed by the molecular sieves. After about 15 minutes the pressure in the system was checked as rapidly as possible ($\sim$ 1 sec). Pumping of the gases by the gauge can become extensive if the gauge is left on much longer.[22] If the pressure was less than 4×10^{-5} torr, the gases were drawn into the sample section by opening valve #4 and placing liquid nitrogen on the charcoal cold finger (1) for 30 minutes. Work at this laboratory has shown that at least 99% of the argon present was removed from the mass spectrometer in 30 minutes when liquid nitrogen was placed on the sample section charcoal cold finger. Since the argon isotopes would all be condensed at the same rate, a small loss during this step should not affect the final results appreciably. After the sample was drawn into the sample section, valve #4 was closed and the liquid nitrogen replaced by warm water for about 5 minutes. The sample was now ready for mass spectrometric determination.

6. Mass Spectrometric Analysis. The mass spectrometer pump valve (#7, Figure 1) was closed and the valve between

the sample section and the mass spectrometer (#6) opened for 4 minutes. Sometime prior to this step a background spectrum was run on the mass spectrometer. There was usually no mass 4, 36, or mass 38 peak observable and only occasionally a small mass 40 peak ($\sim$0.2 to 0.4 mv). The mass spectrometer was then focused on the mass 40 peak and the accelerating voltage turned off.

Estimates of equilibration rates based on the method of Dushman[14] for calculating conductances for high vacuum systems indicated that pressure equilibration should be completed between the sample section and the mass spectrometer in 70 seconds. However, observation of the mass 40 peak from the time of opening the valve indicated that about 3 minutes were necessary for the mass 40 signal to stabilize.

After having been open for 4 minutes to achieve equilibration, valve #6 was then closed, and after an additional minute, the accelerating voltage was turned on and the mass 40 peak was monitored until it had stabilized. The mass 38, 36 and 4 signals were then monitored in a similar manner as rapidly as possible. Scanning all four peaks twice took about 10 minutes. The usual procedure was to use two peaks to extrapolate to "time zero", that is, the time at which the accelerating voltage was turned on, in order to correct for any memory effects, which involved either an increase or a decrease of signal with time. Both effects have been noted at different times and apparently were a function of the recent history of the mass spectrometer.

The procedure used initially in this study involved introducing the sample while the accelerating voltage was on. The reproducibility of the technique was tested by analyzing a gas sample and then drawing the sample back into the sample section (D, Figure 1) with liquid nitrogen. It was later re-analyzed after the mass spectrometer had been pumped down to its usual background pressure ($\sim 1 \times 10^{-9}$ torr). Very poor reproducibility was obtained, with replicates differing by as much as 19%. To determine why this was occurring, a series of determinations were carried out in which the mass 40, 38, and 36 peaks were scanned as rapidly as possible. Figure 4 presents the results from a determination in which the mass 40 and 38 peaks were scanned. It can be seen that there was a wide fluctuation of signal strength with time and that widely varied results could easily be obtained by extrapolating different sets of points back to zero time. Other determinations established that the mass 36 signal behaved in a similar manner. This oscillation was avoided by introducing the sample to the mass spectrometer with the accelerating voltage turned off. A total of 5 minutes was allowed for equilibration, four with valve #5 open and one with it closed. A similar determination (Figure 5) revealed that pumping still occurred, but now the concentration decay curve was smooth and regular. The mass 40 signal was monitored first and then alternately with the other mass signals. The mass 40 signal was extrapolated to time zero and interpolation used to measure mass

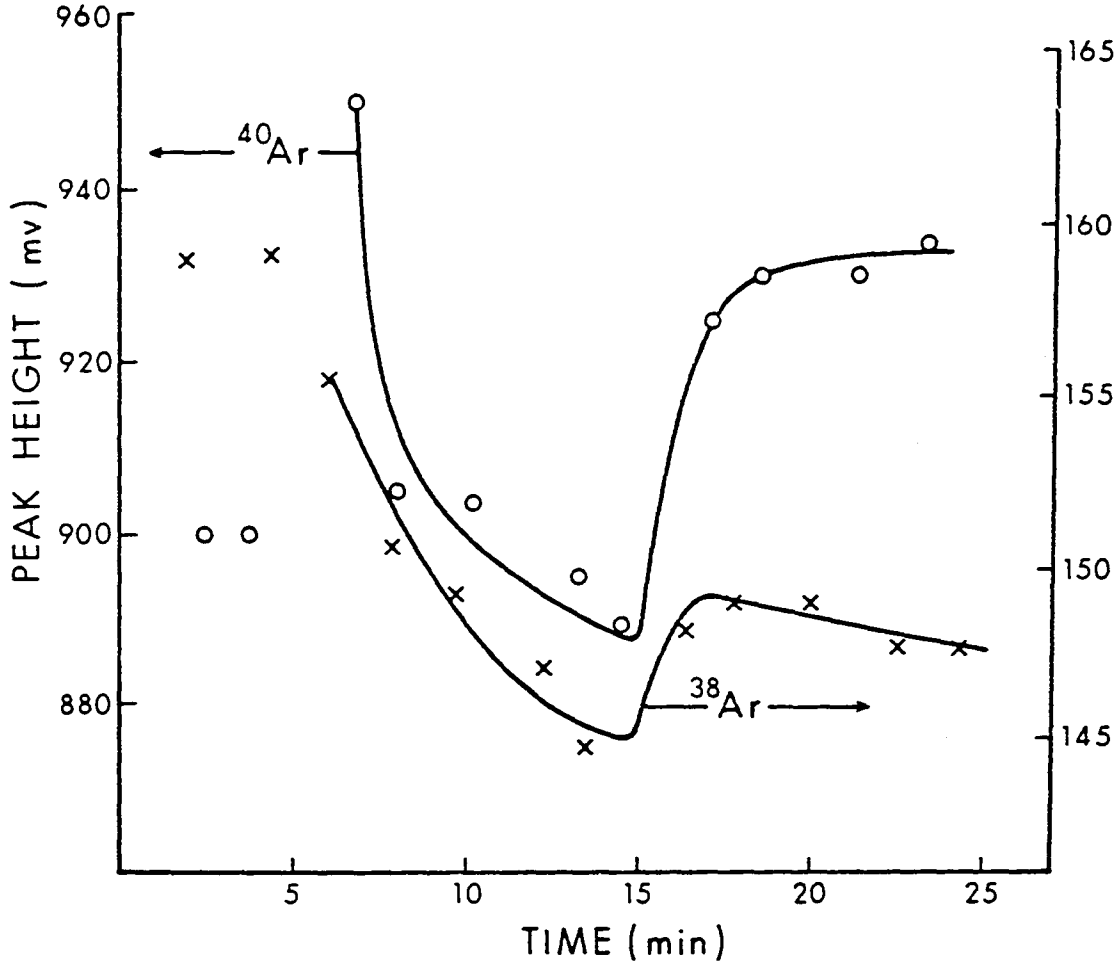

Figure 4

Variation of Argon Peak Height with Time,
Previous Technique

ratios for the other mass numbers since the decay curve was non-linear. This technique gave replicate results that differed by 2.5% at the most. This procedure was used until the mass spectrometer had to be opened to the atmosphere to replace a valve and a Vac-ion pump cartridge and consequently baked out. In subsequent runs it was noted that the mass 40 signal increased slightly immediately after turning on the accelerating voltage and then either increased or decreased slightly in a linear manner. In these runs the mass 40 peak was monitored first and the initial slope used to extrapolate the peak height to time zero. The other mass peaks were monitored in turn and two peaks of each used for extrapolation. No indication of the non-linear memory effect which existed previously for the other mass numbers could be found. The reason for this is not truly understood at this time. However, the replicate determinations usually agreed within 3.0%. In all cases mentioned above, peak height refers to the average signal monitored over a 0.5 to 1 minute interval. For minor constituents, this was necessary to average the noise fluctuations and to make sure the peak maximum had been located.

After each determination the mass spectrometer and sample sections were pumped down using the Vac-ion pumps. The Cu-CuO section was opened to the mercury diffusion pump for a short time and then isolated by closing valves #2 and #4 (Figure 1). The molecular sieve trap (i) in the titanium

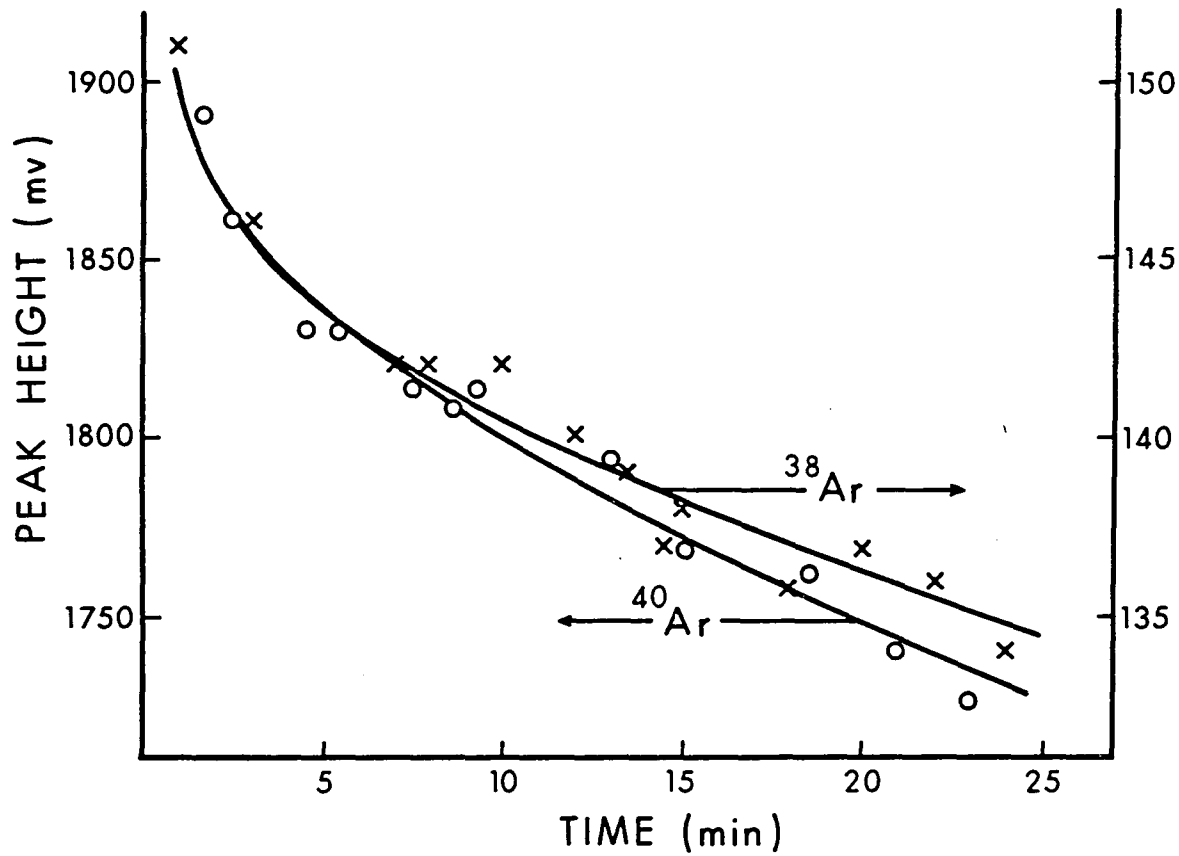

Figure 5

Variation of Argon Peak Height with Time, Present Technique

getter section was degassed by heating for about one hour. The titanium getter furnace was heated to about 840°C overnight. The following day the titanium getter furnace was turned off and the molecular sieve trap heated if a high system pressure indicated this to be necessary. The charcoal cold finger (p) was degassed by heating gently with a torch flame, and after the system pressure decreased to about 2×10^{-6} torr, the ionization gauges were degassed and the system leak tested by isolating it from the pumps. If the pressure remained below 2×10^{-6} torr for five minutes then an aliquot of argon-38 was isolated in the pipette (o) and drawn into the extraction section. A new sample was introduced into the crucible by manipulation of the iron bar and magnet and fused as before. After a crushing run, and after all the samples in the sidearm of one reactor had been fused, the crusher or the reactor was removed from the system under vaccum by collapsing the glass connecting tube with a flame and the crusher or reactor cleaned up in preparation for later determinations. After all the samples had been used, the system was opened and new samples in clean reactors were glass blown into the system. The system was then baked out at approximately 400°C as previously described, in preparation for the next cycle of determinations.

D. Potassium Analysis Procedure

The steps of the "standard" procedure may be summarized as follows:

1. The sample was decomposed with hydrofluoric and perchloric acid and the cations converted to their chloride salts.
2. Salts were dissolved in dilute hydrochloric acid and the necessary solutions were prepared.
3. The apparent potassium concentration of each solution was determined by flame photometry and the actual potassium concentration was calculated by the standard addition technique.

The procedure is described in detail as follows.

The sample to be analyzed was ground to less than 100 mesh size in an agate mortar and a one gram portion weighed into a platinum crucible. Twenty-five cm^3 of concentrated hydrofluoric acid (48% by weight) and 5 cm^3 of 70% perchloric acid was added and the crucibles heated gently on a hotplate overnight. An additional 25 cm^3 of concentrated hydrofluoric acid was then added to the nearly dry crucibles and the mixture heated to dryness over a period of 24 hours. The residue was taken up in 20 cm^3 6N hydrochloric acid and transferred to a 50 ml volumetric flask. In most cases the residue dissolved completely. The crucible was carefully washed with deionized distilled water. Deionized distilled water ($\sim$ 0.01 ppm potassium) was used for all dilutions and for final rinses of all flasks and containers. After diluting the solution to 50 ml, two 20 ml aliquots of each solution were transferred to 100 ml volumetric flasks. To each flask

10 ml of a 150 meq lithium-per-liter solution was added and to one of each pair a known amount of a potassium standard was added. The standard had been prepared by dissolving a carefully weighed amount of pure potassium sulfate in deionized distilled water. Several independent determinations of the potassium concentration of this solution were carried out.

The final sample solutions were stored in polyethylene bottles unless they were to be analyzed in a matter of a few hours.

The solutions were analyzed in groups of four with frequent calibrations. Pure water was aspirated for 2 to 4 minutes between each group of solutions to reduce the chances for salt build-up in the aspirator or spray-chamber. If it was necessary to readjust the lithium photocell output the adjusted setting was used for both of the analyte solutions. The average of at least three readings was used. If a large variation within the three readings was observed it indicated some instrument malfunction. The poor reproducibility was, in every case, eliminated by proper adjustment of the operating conditions.

III. Results and Discussion

Before a detailed discussion of the various aspects of this research is undertaken it may be beneficial to emphasize the qualitative nature of much of the work being reported. The relatively low concentration of inert gases and potassium in the minerals studied lead to a degree of uncertainty not usually encountered in geochronological work. The argon concentrations are 10 to 50 times lower than those encountered in minerals usually used for dating and the potassium concentrations are lower by a factor of about 100. The helium concentrations are similarly low.

As a result, these data have a greater degree of uncertainty than was desired. However, it will be shown that the degree of uncertainty is not so large as to eliminate the possibilities for drawing meaningful conclusions.

A. Accuracy and Precision of Results.

1. Calibration of the argon-38 tracer system.

The accuracy of the radiogenic argon determination is based, ultimately, on the calibration of the argon-38 tracers or "spikes". As pointed out previously, a direct determination of the volume of the added argon-38 is difficult and often inaccurate.

With the pipette system used in this work, the amount of argon-38 in successive tracers decreases since each tracer removes a constant fraction of the gas in the reservoir bulb. The volume (STP) of any tracer may be calculated from

the following expression:[11]

1) $V_x = V_i e^{-\gamma}(x-i)$

where V_x = volume of tracer number x:std cm^3, V_i = volume of tracer number i:std cm^3, and γ is the depletion factor and is equal to the ratio of the pipette volume to the volume of the reservoir bulb plus the pipette. If the log of the tracer volume is plotted versus the tracer number, a straight line with the slope $\frac{\gamma}{2.303}$ should result. An attempt was made to measure the pressure of the argon-38 reservoir at the time it was prepared. Initial calibration runs indicated the tracer volume calculated from the measured pressure were in error by a factor of three so the U.S.G.S. muscovite (P-207) was used as a secondary standard. A known amount of the muscovite was melted and the released gas purified and analyzed. It can be shown that the amount of argon-38 in the tracer can be calculated from:

2) $$^{38}A_V = \frac{^{38}A_H \; k \; w_s}{^{40}A_H^T - {}^{36}A_H R}$$

where the symbols have the following meaning:

$^{38}A_V$ = Volume of argon in tracer:std cm^3

$^{38}A_H$ = Measured height of argon-38 peak:mv.

k = Volume of radiogenic argon-40 per gram of P-207 muscovite

w_s = Weight of muscovite sample, g.

$^{40}A_H^T$ = Measured height of argon-40 peak:mv.

$^{36}A_H$ = Measured height of argon-36 peak:mv.

R = Measured ratio of argon-40 to argon-36 for atmospheric argon

The value of R was measured several times and re-measured periodically by introducing an air argon sample in the same manner as the argon-38 tracer was introduced. A value of 290 was determined initially, but after making minor adjustments in the mass spectrometer operating conditions, the measured argon-40 to argon-36 ratio was 300. This ratio was the average of 7 measurements and was believed to be reproducible to within 3%. The accepted value for atmospheric argon is 296. As mentioned previously, this small discrimination is believed to result from the effect of the fringe field of the mass spectrometer magnet on the ion source. The value k was determined by several different workers[38] and can be assumed to be accurate to within 1%.

The log of the measured tracer volumes and tracer numbers may be plotted and these points used to draw a best straight line with the slope predicted by the measured depletion factor, which for this pipette system was 2.33×10^{-3}. This calibration curve was used to estimate the volume of argon-38 tracers used in radiogenic argon determinations. Figure 3 presents the calibration data obtained from one

argon-38 reservoir and the straight line used for volume estimations. A lease-squares fit of these seven points resulted in a straight line with an intercept of 3.13×10^{-7} std cm^3 and a slope corresponding to a depletion factor (γ) of 2.12×10^{-3}. This compares with the graphically determined intercept of 3.14×10^{-7} std cm^3 and the calculated depletion factor of 2.33×10^{-3}. The standard deviation (relative to the expected value) for these seven determinations and five determinations carried out using a different argon-38 reservoir was 1.3%. An estimation of the probable error for these determinations was made using the following expression:(41)

$$3) \qquad Q = \sqrt{\sum_j \left(\frac{\partial P}{\partial S_j}\right)^2 (q_j)^2}$$

where P is the calculated value, S is the independently measured quantity, and q is the estimated error for each quantity. Individual error estimates used where 1% for the uncertainty in measuring the argon-38 and 40 peaks, 1% for the uncertainty in the amount of argon released (kw_s), $\pm$ 0.1 mv for the uncertainty in measuring the argon-36 peak and 3% for the uncertainty in the argon-40 to 36 ratio. The probable errors range from 1.7 to 3.8% and average 2.2% for the seven samples from the second argon-38 reservoir. A probable error of this magnitude would lead to a standard deviation (σ) of about 3.3% since the probable error should equal 0.674σ. It is not understood why the observed deviation

is significantly lower than that predicted, since the individual error estimates used in the calculation are minimal. Observer bias should not be ruled out as an explanation.

Since the air contamination is at a minimum for the argon-38 calibration runs, and the radiogenic argon determinations are based on these calibrations, the accuracy and precision expected for the radiogenic argon analysis can be no better than that found for the argon-38 determinations.

2. Radiogenic Argon-40 Determination.

A precise definition of the accuracy and precision of the argon determinations is difficult since a large number of determinations were not carried out on any one sample. An estimation of probable maximum error can be attempted using the error expression of Lipson[40]

$$4) \qquad E = \frac{ef}{100 - f}$$

where e = % error in the argon-40 to 36 ratio, f = % air argon in sample, and E = % error in the radiogenic argon determination. This expression is, apparently, an algebraic derivation of the expression for the radiogenic argon in a gas sample:

$$5) \qquad {}^{40}A^{R} = {}^{40}A^{T} - {}^{36}A^{R}$$

where ${}^{40}A^{R}$ = Volume of Radiogenic argon-40:std cm^3, ${}^{40}A^{T}$ = Volume of total argon-40:std cm^3, ${}^{36}A$ = Volume of argon-36:std cm^3, and R = argon-40 to argon-36 ratio. An assumption basic to all these calculations is that all the argon-36

present in the gas is the result of air contamination and that argon-40 to argon-36 ratio of air has not changed since contamination took place. The general good agreement between selected geological and radiogenic dates can be taken as proof of the validity of this assumption.

Equation 4) assigns the significant error in the measurement to the uncertainty inherent in the argon-40 to argon-36 ratio used to correct for the atmospheric argon present in the gas sample. While in most cases this expression affords a reasonable estimate, it ignores the fact that when the argon-36 content of the gas sample is low enough, the ability to measure this isotope may be the limiting factor in the accuracy of the determination. A reasonable estimate of the possible error in the argon-40 to 36 ratio is 3%. If, for example, the noise level of the recording system limits the measurement of the argon-36 peak to $\pm$ 0.1 mv and the argon-36 peak is less than 3.0 mv, then there will be more uncertainty in the measurement of the argon-36 content than that inherent in the atmospheric argon correction. None of the peaks heights could be measured to an accuracy greater than 1%. As a result, the expression for the probable error (Q) for expression 5) becomes:

$$6) \quad Q = \left[\left(\frac{{}^{40}_{A}R}{{}^{40}_{A}T} \right)^2 \left(\frac{{}^{40}_{A}T}{100} \right)^2 + \left(\frac{{}^{40}_{A}R}{{}^{36}_{A}} \right)^2 (\phi)^2 + \left(\frac{{}^{40}_{A}R}{R} \right)^2 \left(\frac{3R}{100} \right)^2 \right]^{1/2}$$

where ϕ = estimated error in the argon-36 measurement and the errors assigned to each factor were as follows: $^{40}A^{T}$, 1%; R, 3%; ^{36}A, 0.1 mv or 1%, whichever was larger. The calculated probable errors are listed in Table III, along with the argon concentrations found for each sample. Figure 6 is a presentation of some of the probable errors plotted against the air argon content of that sample. Also plotted is the probable error estimated from equation 6). It can be seen that most of the probable errors calculated from equation 6) are larger than those predicted by equation 4). While these differences exist rather consistently over the entire range of air contamination, it can be seen that the differences are relatively more important at high air argon concentrations. The larger range predicted for low radiogenic, high atmospheric argon content samples by equation 6) will more likely include zero radiogenic argon content than if equation 4) is used. It is believed that the probable error predicted by equation 6) is the more acceptable of the two. It can be seen that the probable errors cover a wide range but that over half of the determinations have probable errors of 10% or less.

The calculation of the probable error does not take into consideration variables such as differences in successive rock samples from the same specimen and unsuspected irregularities in the extraction and purification procedure. These factors are difficult to assess so the probable errors

Table III

Radiogenic Argon Analyses

Sample	Extraction Method	Atmospheric Argon: %	Probable Error: %	Radiogenic Argon: cc'sx10^{-7}
Dunite nodule, Hualalai, (Figure 9)				
Corner section, HK-160-A	Fusion	56	17	2.44
" " "	Crushing	92	105	0.43
" " "	"	100		
Center of one face, HK-160-C	Fusion	54	7	3.54
" " " " "	"	86	20	3.22
" " " " "	Crushing	82	24	1.27
" " " " "	"	92	42	1.19
Corner section, HK-160-E	Fusion	59	8	2.48
" " "	"	52	7	2.43
" " "	"	60	8	2.11
Center of 2nd face, HK-160-F (contained magnetite)	Fusion	37	6	6.27
" " " " "	Crushing	54	7	5.20
" " " " "	"	64	10	1.80
Center of nodule, HK-160-G	Fusion	30	4	10.68
" " " "	"	27	3	9.41
" " " "	Crushing	37	6	4.31
" " " " 400 mesh	Fusion	71	11	2.96
Outer crust	Crushing	86	39	0.38
Dunite nodule, Hualalai, Center section, HK-161	Fusion	26	3	8.87
Edge section, HK-161	Fusion	18	2	8.37
Dunite nodule, Hualalai, Edge of section taken from center of nodule, HK-166-C	Fusion	30	4	4.27
" " " "	Crushing	100		
" " " "	"	97	77	1.06

Table III (Cont.)

Radiogenic Argon Analyses

Sample	Extraction Method	Atmospheric Argon: %	Probable Error: %	Radiogenic Argon: $cc's x 10^{-7}$
Center of nodule, HK-166-E	Fusion	53	6	3.79
" " " "	Crushing	83	20	2.48
" " " "	"	66	9	1.26
Edge of section taken from center of nodule, HK-166-I	Fusion	27	3	6.29
Large section taken from edge of nodule, HK-166-J	Fusion	63	4	2.69
Dunite nodule, Hualalai,				
Olivine, HK-137	Fusion	81	18	1.99
Feldspar, "	"	43	4	7.63
Pyroxene, "	"	31	17	23.5
Magnetite, "	"	78	13	3.34
Dunite nodule, Hualalai,				
Olivine from edge section, HK-168	Fusion	28	2	15.2
" " " " "	"	24	2	14.6
Iddingsite from edge section, "	"	53	8	2.30
" " " " "	"	70	10	2.19
Olivine inclusion, Salt Lake,				
Olivine, HK-170	Fusion	97	123	0.16
" "	"	94	140	0.53
Pyroxene nodule, Bultfontein,				
Olivine, HK-174	Fusion	90	48	0.73
Pyroxene, "	"	19	3	18.4
" "	"	24	4	17.9

Table III (Cont.)

Radiogenic Argon Analyses

Sample	Extraction Method	Atmospheric Argon: %	Probable Error: %	Radiogenic Argon: cc'sx10^{-7}
Feldspar nodule, Hualalai,				
Center section, HK-167	Fusion	24	2	9.32
" " "	"	34	4	8.89
" " "	"	77	11	8.58
" " "	Crushing	85	31	1.77
" " " 400 mesh	Fusion	100		
Edge section	"	29	3	10.01
Kimberlite inclusion, Salt Lake,				
Biotite, HK-175	Fusion	95	47	8.13
" "	"	77	22	6.17
Deep Ocean tholeiite,				
Whole rock, HK-162	Fusion	49	5	4.65
" " "	"	74	12	1.84
" " "	"	70	9	2.81
" " "	Crushing	97	82	0.42
" " "	"	82	16	0.75
" " "	"	91	42	0.32
" " " 400 mesh	Fusion	92	39	2.02
Olivine, HK-162	Fusion	72	28	1.41
Deep Ocean Tholeiite,				
Whole rock, HK-172	Fusion	70	78	1.63
" " "	"	65	14	1.29
Deep ocean tholeiite,				
Whole rock, HK-173	Fusion	100		
" " "	"	100		

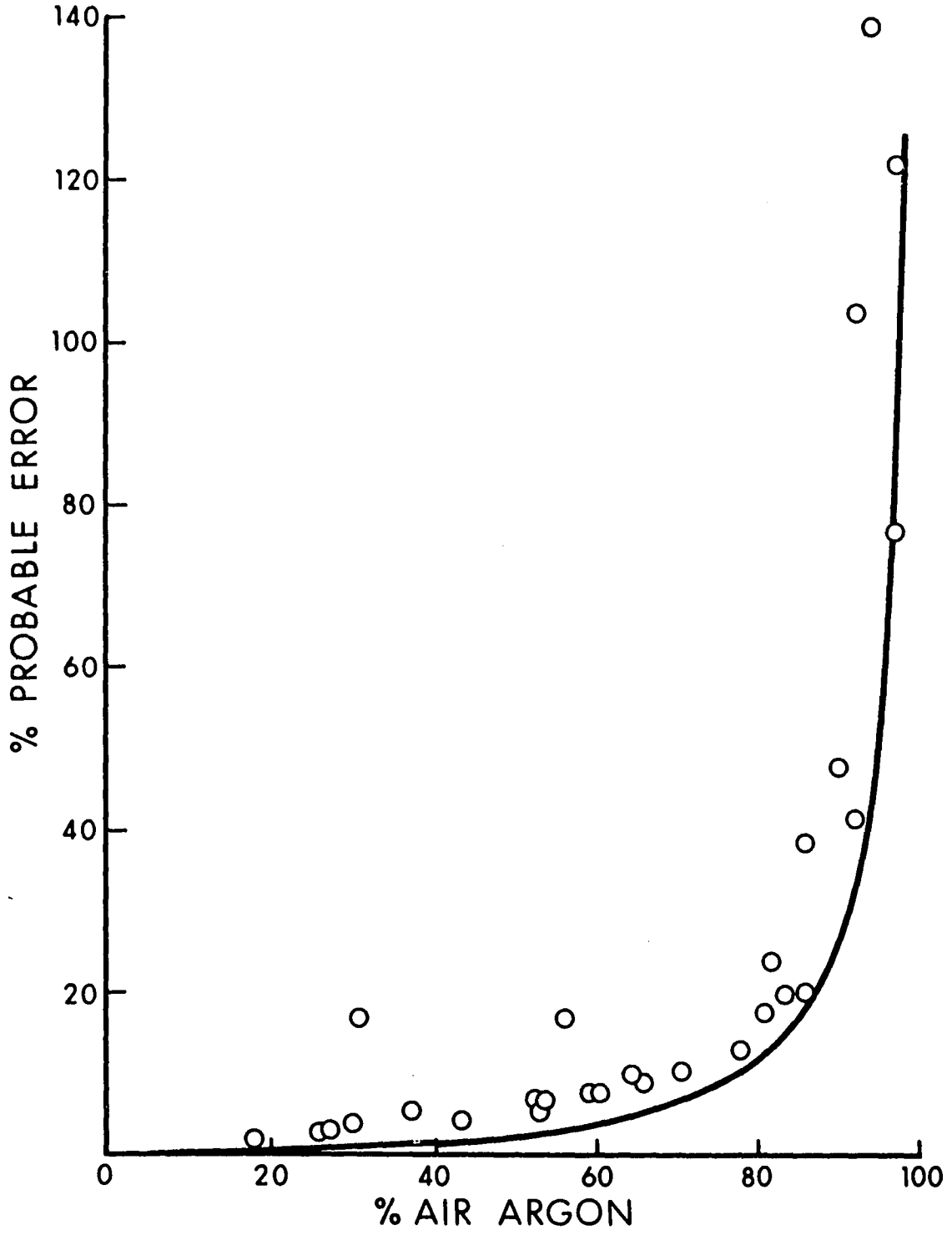

Figure 6

Relation of Calculated Probable Error for Radiogenic Argon Determinations to Air Argon Content of Gas Samples

must be assigned to the particular determination under consideration and regarded as minimal.

Most of the above arguments and conclusions apply to determinations utilizing either the crushing or the fusion technique for releasing the radiogenic argon. The main difference between the two is that in most cases not all the radiogenic argon is released in crushing runs and so the amount of radiogenic argon observed will be a function of the grinding efficiency of the particular experiment. The crushed residues varied in mesh size from 11% by weight smaller than 100 mesh to 28% by weight smaller than 250 mesh. In one experiment the crushing was continued for an additional 16 hours after the analysis of the gas released by the standard 4-hour crushing had been completed. No additional radiogenic argon was detected.

3. Helium Determination.

Since the most likely source of the excess argon present in some minerals appears to be magmatic, and since it is reasonable that helium should occur in magmatic gases as a consequence of radioactive uranium decay, it was believed that an attempt to measure the helium content of the inclusions should be made.

The determination of small amounts of helium in minerals was difficult for three reasons:

1. The relatively high diffusion rate of helium in glass and quartz results in a constant influx of helium

from the air into the vacuum system used for these determinations.

2. The mass spectrometer was relatively insensitive to helium (about 1/20th as sensitive to helium as to argon).

3. A supply of helium -3 tracer was not available. As a result, an extraction blank and a calibration factor had to be calculated to correct the measured helium for helium diffusing into the system during the operation and to convert the output signal (helium peak height) to a helium volume.

Because the apparatus and the procedure used for extraction was changed from time to time, the extraction blanks and the volume dilution factors had to be measured periodically to correct for these variations. For example, early in the work quartz reactors without water jackets were used for the fusions. In these runs, the very large and variable amounts of helium that were detected made quantitative analysis of released helium impossible. Water cooled jackets were later added to the reactors. Relatively low blanks ($\sim 1 \times 10^{-7}$ std cm^3) were then obtained for the fusion runs because the cooled reactor walls ($\sim 100°C$) kept helium diffusion to a minimum. The crushing runs required at least four hours and this resulted in a higher helium blank than that found for the shorter (~ 0.5 hour) fusion runs.

As mentioned previously, it was discovered that the helium blank could be reduced by pumping away the helium in

the argon-38 tracer while the argon was condensed on charcoal at liquid nitrogen temperature. A further reduction was accomplished by measuring the helium content immediately after fusion and before gettering, while the argon was still condensed on charcoal at liquid nitrogen temperature.

Because the helium occupies the entire extraction system and only a fraction of the total gas is taken into the sample section, the calibration depends on the relative volumes of the sample section and the extraction and purification system. The volume of the sample section remains constant but the volume of the rest of the extraction system changes when a reactor or the crusher is removed after use. To correct for this effect the volume of the extraction and purification sections, reactors, and crusher must be known. Accurate measurements of the volumes of the reactors, crushers, getter cans, gauges, and traps could be made by filling them with water when they were not in use. These accounted for about 85% of the total volume. The tubing volume was estimated by measuring the length and diameter of the accessory tubing and calculating the volume. The correction factors were then simply a ratio of the volumes estimated for the system with and without the crusher and with and without one reactor. The factors were 0.97 and 0.85 respectively.

The helium calibration factor was determined by analyzing a zircon sample (M.I.T. R-1659) kindly made available

by Dr. Damon of the University of Arizona that had been previously analyzed by Damon and Hurley[12] and by Hurley.[33] The suggested value of 9.26×10^{-5} std cm^3 per gram was used in calculating the factor used for converting peak height in millivolts to std cm^3 of helium. The calculated conversion factor was 1.70×10^{-7} std cm^3 per millivolt. This was the average of three determinations that ranged from 1.51 to 1.85×10^{-7} cm^3/mv. This compares with a conversion factor of $(1.86 \pm 0.19) \times 10^{-7}$ std cm^3/mv obtained through the use of a Veeco (Vacuum-Electronics Corp., Plainview, Long Island, N.Y.) helium source, (Model SC-4, Calibrated Leak). Since a tracer was not used the degree of accuracy and precision is rather difficult to assess. These factors are related to the reproducibility obtained in the operation of the analysis system. In the argon determination the use of the argon-38 tracer compensates for minor day to day variations in the sensitivity of the analysis system. The term "sensitivity" is here defined as the output signal per volume of gas introduced into the mass spectrometer. Since the mass of the argon-38 tracer is in the middle of the argon isotope range it is reasonable to assume that sensitivity fluctuations for argon-40 and argon-36 will be nearly identical to those for argon-38.

As a result, quantitative calculations are possible since the amount of argon-38 is known and the peak heights can be readily measured. Since a helium -3 tracer is not

available the assumption must be made that sensitivity fluctuations are the same over the entire mass range. An experiment was carried out in which the sensitivity of the mass spectrometer was varied by adjusting the trap current and case voltage at the ion source. Peak heights for the argon-40 and helium 4 in one gas sample were measured at each set of conditions. The maximum difference of the ratios of peak heights for each isotope measured at two different sensitivities was found to be about 8%. The amount of helium present is calculated from the following expression:

$$7) \qquad He_v = He_H \times f_c \times \frac{^{38}A_v}{^{38}A_H} \times \frac{^{38}A_H}{^{38}A_{v\ c}}$$

where He_v = Volume of helium:cm^3; He_H = helium peak height: mv; f_c = average response factor for helium measured in calibration runs:cm^3/mv; $^{38}A_v$ = volume of argon-38 tracer: std cm^3; $^{38}A_H$ = argon-38 peak height:mv.

Since this assumes no variation in relative sensitivity over the entire mass range, and measurements have shown an 8% variation can exist, the 8% would be a reasonable estimate for expected precision of the measurement. It should be pointed out that minor fluctuations in the sensitivity are also related to total gas pressure in the mass spectrometer tube. This factor, plus the fact that some of the parameters associated with these fluctuations, the case voltage and trap current, are difficult to measure accurately

make it impossible to quantitatively correct for these fluctuations at the present time.

The accuracy of the helium determination is very difficult to assess since the standard used for calibration has not been extensively investigated. The precision of the measurements is also difficult to determine since only two paired helium determinations were successfully carried out. The crushing runs varied in efficiency so the precision for runs of this type would be expected to be lower. The helium blank correction is known to a maximum precision of $\pm$ 10% and since the released helium is the difference between that calculated from equation 7) and the blank, a probable error may be estimated in the same manner as those calculated for the radiogenic argon. The probable errors are presented in Table IV along with the measured helium concentrations. Figure 7 presents a plot of calculated percent probable error versus percent blank correction. As would be expected, the curve is asymptotic with a lower limit of about 8%.

4. Potassium Analysis.

The analysis of low level potassium in minerals, while often an interesting and challenging problem, was nonetheless not a factor of overriding importance in this study. Since the potassium-to-argon ratios measured in inclusions apparently cannot be used to estimate a true age, the main interest in the potassium concentration was related to its

Table IV

Helium Analyses and Helium-to-Argon Ratios

Sample	Extraction Method	Blank Correction %	Probable Error: %	Helium Content: $cc's x 10^{-7}$	He/A Ratio
Dunite nodule, Hualalai,					
Center of one face, HK-160-C	Fusion	15	10	3.11	0.97
" " " " "	Crushing	61	26	0.96	0.81
Center of 2nd face, HK-160-E	Fusion	26	11	1.55	0.73
Center of nodule, HK-160-G, 400 mesh	Fusion	32	13	1.34	0.45
" " " "	Crushing	26	11	3.49	0.81
Crust, HK-160	Crushing	63	28	0.76	2.00
Dunite nodule, Hualalai,					
Edge of section taken from center of nodule, HK-166-C,	Fusion	14	9	2.81	0.66
" " " "	Crushing	34	13	1.38	
" " " "	"	47	18	0.91	1.30
Center of nodule, HK-166-E,	Fusion	40	15	4.70	1.24
" " " "	Crushing	44	16	4.00	1.61
" " " "	"	26	11	2.00	1.59
Edge of section taken from center of nodule, HK-166-1	Fusion	9	9	4.55	0.72
Large section taken from edge of nodule, HK-166-J	Fusion	13	9	2.86	1.06
Dunite nodule, Hualalai,					
Olivine, HK-137	Fusion	31	13	1.51	0.76
Feldspar, HK-137	"	73	40	0.25	0.03
Pyroxene, HK-137	"	9	9	6.91	0.29
Magnetite, HK-137	"	46	17	0.83	0.25

Table IV (Cont.)

Helium Analyses and Helium-to-Argon Ratios

Sample	Extraction Method	Blank Correction %	Probable Error: %	Helium Content: cc'sx10^{-7}	He/A Ratio
Pyroxene nodule, Bultfontein,					
Olivine, HK-174,	Fusion	20	10	3.56	4.88
Pyroxene, "	"	3	8	26.3	1.43
Pyroxene, "	"	3	8	28.3	1.53
Olivine inclusion, Salt Lake,					
Olivine, HK-170	Fusion	57	23	0.34	2.13
Olivine, "	"	31	12	0.38	0.72
Feldspar nodule, Hualalai,					
Center section, HK-167	Fusion	81	60	0.16	0.02
" " " 400 mesh	"	96	288	0.18	
Kimberlite inclusion, Salt Lake,					
Biotite, HK-175	Fusion	91	140	1.13	0.18
Deep ocean tholeiite,					
Whole rock, HK-162	Fusion	82	63	0.74	0.40
" " "	"	35	14	0.76	0.27
" " " 400 mesh	"	82	62	0.15	0.07
Olivine, HK-162	"	46	17	1.41	1.00
Deep ocean tholeiite,					
Whole rock, HK-173	Fusion	20	10	6.63	
" " "	"	12	9	3.11	

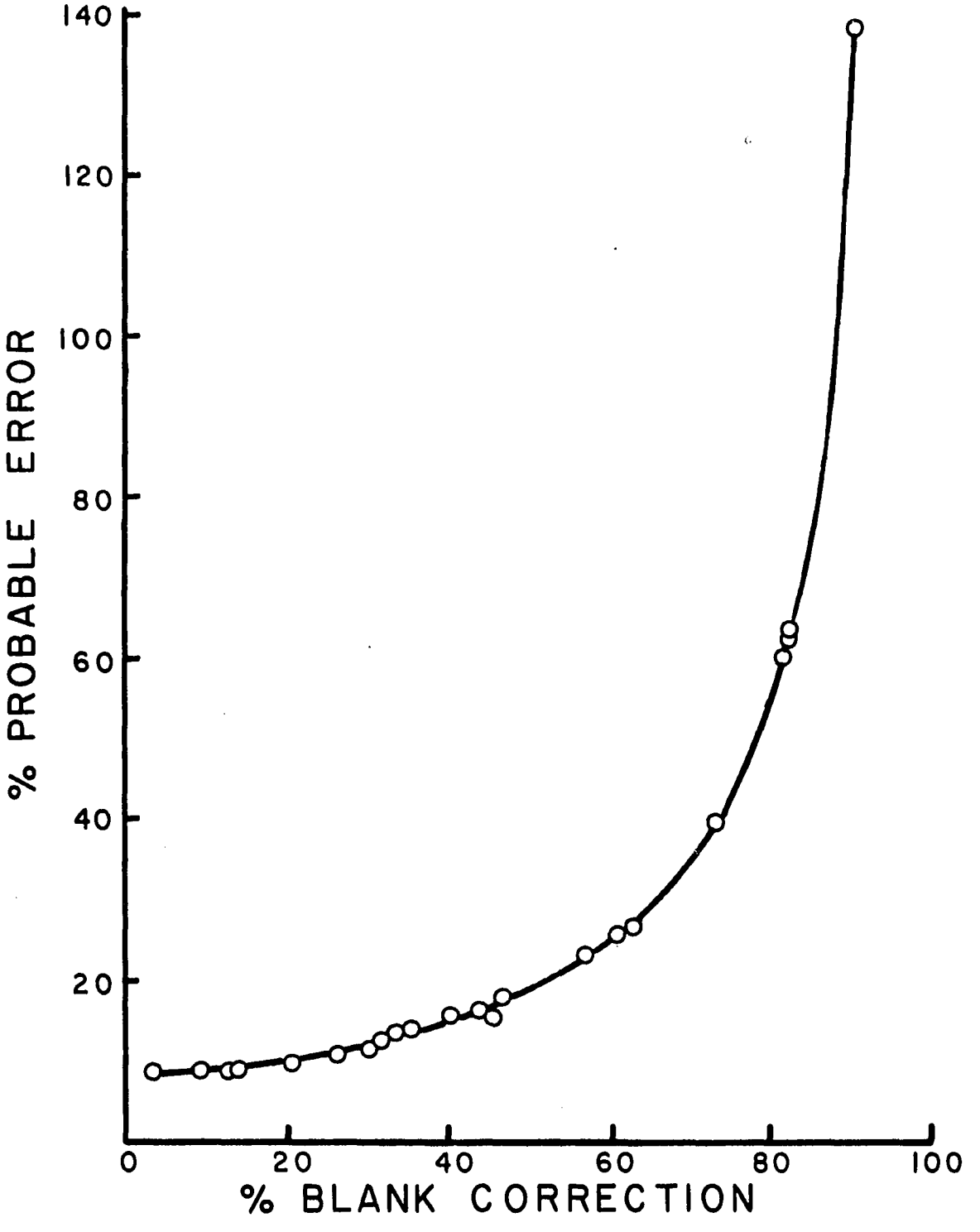

Figure 7

Relation of Calculated Probable Error for Helium Determinations to the Blank Correction

location in the minerals. Analysis of a relatively crude nature will suffice to determine whether or not concentration gradients exist for potassium similar to those found for argon.

The analysis of low level (less than 0.2%) potassium in minerals has been the subject of much research, especially in relation to the age determinations made on meteorites. The book "Potassium Argon Dating" contains an excellent review by O. Muller[50] concerning the commonly used potassium analysis techniques. There was little mention, however, of the analysis of potassium in olivines. The article pointed out that the two most suitable techniques for low level potassium analyses are mass spectrometric isotope dilution analysis and neutron activation analysis. The equipment necessary for neutron activation analysis is not available at this lab. The analytical techniques investigated are discussed below.

1. Solid State Mass Spectrometry. A small solid-state mass spectrometer had previously been constructed and used at this laboratory for the analysis of minerals with potassium contents of 1% and greater. In this technique the sample was decomposed and dissolved in the usual manner and a known amount of a potassium -41 tracer added as a chloride solution. Iron, aluminum, magnesium, calcium, etc., were then precipitated by adding ammonium carbonate and the filtrate evaporated and calcined at 600°C. The sintered

mass was then washed with water and a portion of the filtered solution transferred to a filament which was mounted in the mass spectrometer. A comparison of the measured potassium-41 peak to the potassium-39 peak allowed calculation of the potassium level in the original sample. A decided advantage of this technique was its sensitivity and the fact that the presence of the potassium-41 tracer during sample treatment automatically corrected for concurrent losses of original potassium. A disadvantage was that the procedure was time consuming in that each determination involved assembling and dismantling a vacuum system. The instrument was not used for this reason and also, because reproducible results could not be achieved. It was believed that an unwarranted amount of time would have been needed to adopt this technique to the analysis of olivines.

2. X-ray Fluorescence Spectrometry. An attempt was made to measure the potassium level of a powdered olivine sample by vacuum X-ray fluorescence spectrometry utilizing a chromium target and sodium chloride and pentaerythritol crystals. However, no potassium peak was detected.

3. Flame Photometry. Flame photometry is not usually used for potassium analysis of minerals containing less than 0.2% potassium. Previous work at this laboratory[22] had indicated that the lower limit of the available Beckman D.U. flame photometer was of the order of 0.1 ppm potassium. The equipment available and the amount of reagents required

for sample treatment dictated a maximum sample of one gram and a final solution size of 50 to 100 ml. Under these restrictions, dissolving a typical olivine sample would have resulted in a solution containing 0.3 to 0.5 ppm potassium. Hence, it was believed that if flame photometry were to be utilized, a more sensitive instrument would be needed. The filter flame photometer previously described was kindly made available for our use by Dr. C. Folsome of the Microbiology Department of the University of Hawaii. Initial experiments indicated that the sensitivity of the instrument for dilute solutions was approximately 0.02 ppm. This instrument was designed for use with the internal standard technique. The lithium-potassium pair is one of the most favorable for use with the internal standard technique and since this technique minimizes errors resulting from variation in viscosity and surface tension and, to a lesser extent, from interfering ions it was believed that this would be the most favorable approach using flame photometry. A requirement of this technique is that the concentration of the internal standard element be low in the sample being analyzed. While this requirement was satisfied for olivine it should be pointed out that the subsequent use of the standard addition technique greatly reduced the effect of any lithium present in the rock sample on the final calculated concentration. It was found that the high concentration of chloride ion present in the analyte solutions often

resulted in severe repression of the lithium radiation. When this happened, manual adjustment of the lithium photocell output was necessary. This invalidated the calibration procedure usually used and necessitated either a set of standards with a similar iron, magnesium and chloride level or the use of the standard addition technique. Since the variability of the concentrations of the interfering ions was large and difficult to control it was believed the standard addition technique was necessary to achieve the desired level of accuracy and precision. As a result, the procedure finally adopted was not truly an internal standard technique.

Olivine is soluble, with difficulty, and has a high concentration of iron and magnesium. An effort was made to dissolve the sample in a minimum of solvent so that the resultant anion concentration would be as low as possible and also to minimize the blank resulting from potassium in the reagents. Dilute hydrochloric acid was chosen as the final solvent since Dean[13] had reported that higher concentrations of chloride may be tolerated than of sulfate, nitric, or phosphate and because very pure hydrochloric acid could be obtained by a simple distillation. For these reasons, the metal ions were converted to the chloride salts after the decomposition of the minerals by hydrofluoric acid treatment.

Before the "standard" procedure was adopted, two separate attempts to discover a technique for removal of the

interfering cations, mainly iron and magnesium, were made.

The first attempt involved precipitation with carbonate in presence of excess sodium ion. It was hoped that the sodium would occupy the sites in the precipitate that would otherwise adsorb potassium ions. With a 250 to 1 sodium-to-potassium ratio during precipitation, 50% of the potassium present was not recovered. Since the interfering ions are present in excess of the potassium by 5000 fold and there could be one site per precipitate ion, it was believed that the problems of sodium interference and sodium reagent purity would be acute if enough sodium ion were added to reduce potassium adsorption to a negligible level.

An attempt was also made to remove the iron and magnesium by chelation with 2,4 pentanedione. While some success was achieved, it was apparent that an unwarranted amount of time and effort would be needed to develop this technique properly.

The results of the potassium analyses are presented in Table V. It can be seen that the precision is rather poor. Only a few determinations were carried out on the higher potassium content rocks. However, it was felt that these determinations were accurate to ±5%. The accuracy of the olivine analyses is harder to assess; however, the averages are probably accurate to about ±30%. The poor precision of these determinations precluded obtaining any meaningful results in regard to the fraction of the potassium recovered.

Table V

Potassium Analyses

Sample	Potassium Concentration: PPM Individual Results	Average
HK-160-G[a]	42, 20, 28, 45	34
HK-160-C[a]	48, 98, 50	65
HK-166-J[b]	97, 73, 103	91
HK-166-C[c]	65, 42, 50	52
HK-160-E[a]	390, 383	387

a - See Figure 9.

b - Edge section of dunite nodule.

c - From center section of dunite nodule.

An attempt was made to measure the potassium released from samples by crushing. If the small amounts of potassium found in olivines are not present in the lattice but rather in fluid inclusions, then a crushing technique that would release argon would probably also expose potassium so that it could be extracted by merely rinsing the crushed mineral with water. Several attempts were made to measure released potassium in this way and potassium was detected in the rinse water, using the lithium internal standard technique for analysis. However, subsequent experiments indicated that the crushing apparatus had easily removed potassium that could not be eliminated by normal cleaning methods. Whether the potassium was being leached or scraped from the crucible, or remained from previous runs was not known.

B. Calculation of Potassium-Argon Ages.

1. Method of Calculation.

The potassium-argon age can be calculated from the following expression:[22]

$$8) \quad t = \frac{1}{\lambda} \ln\left(1 + \frac{1 + R}{R} \quad \frac{^{40}A_{rad.}}{^{40}K} \right)$$

Where t = age,

$\lambda = \lambda_{B-} + \lambda_K$ = total decay constant,

λ_{B-}, λ_K = decay constants for the decay of ^{40}K to ^{40}Ca and ^{40}A respectively,

$R = \frac{\lambda_K}{\lambda_{B^-}}$ = branching ratio for the double decay of ^{40}K,

and $^{40}A_{rad.}$, ^{40}K = number of atoms of radiogenic argon 40 and potassium -40, respectively.

Equation 8) can be derived from the expression for the concurrent first order decay of a substance to two products. The age will be correct if no diffusion losses of parent or daughter elements have taken place and the initial argon-40 concentration was zero. An interesting history of the discovery of the decay paths and their respective decay constants has been presented by F. G. Houtermans[32] and need not be repeated here. However, it should be pointed out that the most reliable value of the decay constants for ^{40}K obtained by geological methods[3] agrees within one percent with those obtained by counting.[16] The values used in these calculations were $\lambda = 5.32 \times 10^{-10} y^{-1}$ and $R = 0.123$. Replacing ^{40}K with K_{total}, using 0.0119% as the isotopic abundance of ^{40}K, converting $\frac{^{40}A}{K}$ to std cm^3/g and using common logarithms, results in the following equation:

$$9) \quad t_{m.y.} = 4320 \log \left[1 + 134.7 \frac{^{40}A_{rad.}}{K_{total}} \right].$$

For small values of t (< 30 my) the expression

$$10) \quad t_{my} + 2.53 \times 10^5 \times \frac{^{40}A_{rad.}}{K}$$

will serve as an approximation with an error of less than one percent.

2. Measured Ages.

Comparison of the amounts of radiogenic argon extracted by the crushing technique with that extracted by the fusion technique (Table III) from the same sample shows that the crushing technique can release significant amounts of radiogenic argon from most of the samples investigated in this study. While the effect of grinding on the release of argon from the crystal lattice is not fully understood, it is agreed by workers in the field that excessive grinding will release some lattice argon but that a sample grain size of 100 mesh is probably a safe practical lower limit[5] for samples to be dated. Much finer material has been dated successfully, however.[17] In most of the crushing experiments carried out in this study 50 percent of the crushed material was greater than 100 mesh when the crushing was halted. It is probably safe to assume that most of the gases released in this way did not come from the crystal lattice. If one makes the rather tenuous assumption that all of gas not held in the crystal lattice was released by crushing and that it was not associated with the measured potassium, then a calculation of an apparent age is possible by subtracting the amount of gas released by crushing from the total released by fusion. Ages calculated in this manner are presented in Table VI. Also presented are the apparent

Table VI

Apparent Helium and Argon Ages

Sample	Argon Released (STP cc's x 10^7) By Fusion[a]	By Crushing[a]	Potassium: PPM	Apparent Ages (my) Calculated Using: Gas Released by Fusion	Difference between Gas Released by Fusion and Gas Released by Crushing
Dunite nodule, Hualalai, HK-160					
Center of nodule-G	10.05	4.31	34	3000	2200
" " " "	2.96		34	1500	
Center of one face-C	3.32	1.23	65	1000	700
Dunite nodule, Hualalai, HK-166					
Edge of section taken from center of nodule-C	4.27	1.06	52	1400	1130
Large section taken from edge of nodule-J	2.69		91	808	
Dunite nodule, Hualalai, HK-137					
Pyroxene	37.1	10.5	134[b]	3000	2400
Feldspar nodule, Hualalai, HK-167					
Feldspar	8.93	1.77	3000	70	130[c]
" 400 mesh	0.0				
Kimberlite nodule, Salt Lake, HK-175, Biotite	6.17		(6.57%)	2.38±0.52	
"	8.13		(6.57%)	3.1 ±1.5	
Deep ocean tholeiite, HK-162					
Whole rock	3.10		(0.37%)[d]	22	

Table VI (Cont.)

Apparent Helium and Argon Ages

Sample	Helium Released (STP cc's x 10^7) By Fusion[a]	By Crushing[a]	Uranium: PPM	Apparent Ages (my) Calculated Using: Gas Released by Fusion	Difference between Gas Released by Fusion and Gas Released by Crushing
HK-137 Pyroxene	6.9		0.01[e]	300	
HK-160-C	3.11		0.0065[e]	211	
Olivine inclusion, Salt Lake,					
HK-170 Olivine	0.36		0.005-0.01[f]	160-320	
HK-137 Olivine	1.51		0.004-0.009[f]	75-166	
HK-167 Feldspar	0.16		0.3[e]	0.2	

a - average
b - Funkhouser and Naughton, in press
c - used k = 1310 PPM, obtained after grinding and washing, see page 79
d - reference 49
e - estimated from $K/U=10^4$
f - reference 58

ages calculated on the basis of the total argon released. These ages are all significantly older than the ages assigned to the formations in which these inclusions were found.

If the gas released by crushing is inherited argon and the remainder is the result of radioactive decay of the potassium in the rocks, then the ages calculated in the above manner can furnish a minimum age for these inclusions. An attempt can be made to correct the apparent ages for diffusion effects using the approach suggested by Wasserburg[60] and by Fechtig and Kalbitzer.[20] In using this method a diffusion coefficient was estimated by extrapolating Amirkanoff's data[4] for argon in pyroxene to 1100°C and an average particle size of 1 mm assumed.[61] The "corrected" ages thus calculated are impossibly old.

If the production rate for argon from potassium and the estimated diffusion coefficient, D (1×10^{-10} cm^2 sec^{-1}) are converted to units of std cm^3 of argon per particle per second, and the particle assumed to be spherical and 1 mm in diameter the diffusion rate is seen to be so much greater than the production rate (6×10^{-15} cm^3 $particle^{-1}$ sec^{-1} versus 3×10^{-27} cm^3 $particle^{-1}$ sec^{-1}), that it is surprising that any argon is found in the mineral. The error in the estimated diffusion coefficient would have to be large to change this deduction. The above leads to the conclusion that the argon found in these minerals is there as a consequence of a relatively high magmatic argon partial pressure.

It is possible that some of the argon originated within the mineral and the argon partial pressure in the magma was high enough that a steady state condition was achieved. Because of the prevalence of fluid inclusions in these minerals, it seems more likely that most of the argon produced in the lattice has diffused out of the mineral or into its fluid inclusions and that most of the argon found in the mineral is from the environment and has been trapped in fluid inclusions as a result of the annealing and closure of microcracks.

Funkhouser[22] has estimated that an argon partial pressure of 30 to 300 torr could exist in the magma chamber. This conclusion was based on the estimated amounts of water and argon in the hydrosphere, the atmosphere, and on the estimated amount of water in the magma. If one applies the same reasoning to helium, however, the resultant helium-to-argon ratio is 6×10^{-4}. This is clearly not in line with the results obtained in this study.

The foregoing leads to the conclusion that the argon which is normally assumed to be held in the crystal lattice of the minerals (Table VI) is more probably located in fluid inclusions or trapping sites in the nodules investigated here. "Trapping sites" is here taken to mean a site that is probably a collection of vacancies. As a result, the diffusion coefficient would be entirely different than that proposed by Amirkanoff[4] for argon in pyroxene. If

the gas is located in fluid inclusions, the only case in which a meaningful age could be calculated would be if the gas had its origin under the following conditions: (1) that all the argon in the mineral was the radioactive decay product of potassium present in the mineral lattice or the fluid inclusions, and either originated within the fluid inclusions or migrated to these sites; (2) that the rate of diffusion of argon out of the inclusion was much lower than the assumed diffusion rate for the argon in the lattice; (3) that no additional argon from the environment was trapped in healing microcracks.

These suppositions are rather difficult to support except in an indirect way. MacEvan and Stevens,[46] after investigating the diffusion of xenon in uranium dioxide, concluded that the variable diffusion rates observed could be best explained by the presence of trapping sites on a submicron basis. They used expressions developed by Hurst[35] to estimate the number of sites and cited the shape of the curve obtained by plotting the fraction of the gas released versus the square root of time as proof of the presence of trapping sites. Such traps can be observed in sinters of uranium dioxide and may be analogous to the fluid inclusions sites found in many ultrabasic inclusions.

In an effort to gain information on the nature of the primitive inert gas environment in volcanic systems, analysis was made of gas released from lavas erupted on the deep

ocean floor which presumably would have undergone negligible degassing. The samples (HK-162, 172, 173) were furnished by Dr. J. G. Moore.[49] They were dredged from the east Kilauea rift zone at depths of from 1400 to 4680 meters off the coast of Hawaii, Hawaii. Moore has described these samples as being from historic eruptions (within the last 200 years) and their fresh appearance supports this view. An age of 22 my (Table VI) calculated for sample HK-162, is clearly incompatible with the geochronology of the area, and suggests that a great deal of caution should be exercised when using submarine materials for dating. The fact that the argon content of the 400 mesh sample was similar to that found for the whole rock is somewhat surprising in that the olivine and feldspar samples lost a large fraction of their argon as a result of grinding. However, since glass is not a highly ordered material it is reasonable to assume that it would be less likely to form long microcracks along crystal planes that could release gas entrapped in the interior of a particle. In other words, the less ordered glass would hold the gases more evenly distributed in the structure (effectively in solution) and would have to be crushed to a smaller particle size to release a majority of its included gases.

Table VI also includes apparent ages calculated for a feldspar from Hualalai. A relatively small fraction of the total argon was released by crushing and the ages were low

compared to those calculated for the olivines. Amirkanoff[4] has reported that he was able to obtain concordant ages for feldspar and mica from the same formation by removing what he called the unstable potassium. His argument was that the low ages obtained for the feldspars in question were the result of lost argon and that if the feldspar structure had opened enough to allow argon to escape the associated potassium must also be in an exposed position. He removed all but the stable potassium ($\sim$70% of the total) by treating the mineral in the presence of a saturated solution of thalium nitrate for six hours at $\sim$500° under the pressure developed by the closed system. He did not state why he chose this technique or if other, more obvious, approaches had been unsuccessfully explored. The equipment needed for the above treatment was not available so a crushed sample was treated with a saturated sodium chloride solution at 80°C for 24 hours, washed, dried, and analyzed for potassium. Fifty-four percent of the potassium was removed by this treatment. The apparent age calculated by using the difference between the two argon determinations and the "stable" potassium was 0.13 my. A great deal more work would have to be done with this technique to draw any definite conclusions, but the approach does hold some promise. The low potassium concentration of olivine precludes applying this technique to such inclusions until a suitable potassium analysis has been developed.

An age of about 2.4 my (Table VI) was calculated for a biotite that had been separated from kimberlite inclusions from the Salt Lake area on Oahu. It is fairly well established[62] that the formation from which these inclusions were taken are no older than 150,000 years. The old age found might be regarded as the result of inherited argon, as in the case of the olivines. However, since biotite is a relatively low melting mineral it is likely that the mineral would redissolve if it were held in the magma for any length of time. The presence of eclogite facies minerals, including garnet, in the kimberlite suggests the inclusion was crystallized at some depth. The low number of observable fluid inclusions[23] and the agreement of the age with that found for the primary Oahu eruptive sequences[57] (2.2 - 3.7 my) suggests that the age may not be due to inherited argon and may be a "true" age. A mechanism proposed by R. Moberly[48] involves the crystallization of the mineral at depth during a previous eruptive series (Koolau Volcanic Series, about 3 my[35]) without ejection from the volcano. If the remaining magma crystallized the mineral would not redissolve and so probably would not lose argon due to a sustained high temperature. The inclusion could be subsequently ejected in the later Salt Lake eruption without any significant loss of argon if it was carried out and deposited rapidly by that later magma.

It is interesting to note that most of "excess" radiogenic ages reported are less than the accepted age of the earth. While most workers do not regard these as true ages and usually assume the "excess" argon had been incorporated into the mineral during its formation, the information used to support these views is largely circumstantial. While, on one hand, it is possible that some mechanism was involved in this incorporation that resulted in a level of argon that just coincidently is low enough for the calculated ages to be less than that of the earth; on the other hand, the fact that crushing releases argon cannot be considered conclusive evidence for its location in fluid inclusions. Since the potassium ion is much different in size than the iron or magnesium ions of the orthosilicate lattice of olivine, for example, it can be argued that the potassium does not occupy true lattice positions and may be located at lattice dislocations or vacancies. These lattice dislocations and vacancies may act as traps for the argon generated at these sites. If this were the case one can visualize that the diffusion coefficient for argon might be higher than expected, but that the argon would be likely to be released during crushing since fracturing would be more likely to occur along dislocations or any strains in the lattice. The obvious weakness with this argument is that it seems just as likely that argon located in lattice dislocations or vacancies would diffuse from the crystal more easily than if in a

true lattice position. Since so little is known about this aspect, however, the mechanism should not be dismissed completely.

C. Calculation of Helium Ages.

Helium ages may also be calculated from the data at hand if a few assumptions are made. The following approximation:

11) $He = (1.20\ U + 0.29\ Th)\ t \times 10^{-7}$

may be derived from the decay laws and the approximate decay constants.[60] Where He = volume of helium produced in t years:std cm^3/g; U = concentration of uranium:g/g; Th = concentration of thorium:g/g; and t = time:my. If a thorium-to-uranium ratio of 3.7 is assumed[58] and uranium analyses for similar minerals applied to the specimen investigated in this study, the helium ages listed in Table VI may be calculated. The helium ages are in every case lower than those calculated from the potassium argon data. Even if the estimated uranium concentrations are in error by a factor of 10, which is unlikely,[42,43,64] the helium ages are definitely less than the argon ages and also are excess ages in the sense that they are older than the known date of eruption for these samples. The most obvious explanation is that helium was included during formation or at some later stage and its concentration, therefore, bears no recognizable relationship to its age and uranium content.

D. Estimation of Ages from the Helium-to-Argon Ratio.

Zartman, Wasserburg, and Reynolds[64] have pointed out that the uranium, thorium and potassium contents of "average" rocks can be estimated to a degree of accuracy that will allow assumptions to be made in regard to the helium-to-argon ratios found in natural gases. They used the following relationships to estimate the ratio of gases produced over the past few million years:

12) $$N_{He} = (1.20\ U + 0.29\ Th)\ t \times 10^{-7}$$

13) $$N_A = 3.99\ K\ t \times 10^{-12}$$

where N_{He} and N_A are the std cm^3 of helium and argon, respectively, produced by radioactive decay in a time interval, t, and U, Th, and K are the weights of uranium, thorium, and potassium, respectively, in grams. For longer periods of time the calculations must be based on the respective decay laws since the above approximations will not be accurate for periods much longer than 30 million years. The following expressions were used to calculate the amount of gas produced in the interval, t years:

14) $$He_v = 22.4 \times 10^3 \sum_j k_i N_i\ (e^{\lambda_i t} - 1)$$

where He_v = volume of helium produced in time t:std cm^3, k_i is the number of moles of helium produced per mole of uranium or thorium, N_i is the number of moles of radioactive

parent per gram of "average" rock and λ_i is the decay constant for each of the following three helium producing reactions:

$$^{238}U \rightarrow {}^{206}Pb + 8\ He, \qquad \lambda = 1.54 \times 10^{-10}\ yr^{-1}$$

$$^{235}U \rightarrow {}^{207}Pb + 7\ He, \qquad \lambda = 9.71 \times 10^{-10}\ yr^{-1}$$

$$^{232}Th \rightarrow {}^{208}Pb + 6\ He, \qquad \lambda = .499 \times 10^{-10}\ yr^{-1}$$

The volume of argon produced was calculated from:

$$15) \qquad A_v = 7.42 \times 10^{-3}\ K\ (e^{\lambda t} - 1)$$

where K is the potassium concentration in grams per gram of rock, t is the time in years, and λ is the total decay constant. The estimates by Zartman, et al.[71] of average rock concentrations of 3.5 ppm uranium, 10 ppm thorium and 2.6% potassium were then used to calculate helium and argon productions per gram of average rock for various time intervals. If the age of the earth is approximately 4.5 billion years, then we would expect average rock to have produced gas with a helium-to-argon ratio corresponding to a time interval of 4.5 billion years. Examination of Figure 8, a plot of helium-to-argon ratio versus time interval, t, will show that this ratio is about 2.8, not 6.8 as proposed by Zartman, et al. The calculations were extended to intervals longer than the "life" of the earth and revealed that the expected ratio would increase for intervals longer than

about 6×10^9 years. There are many factors involved that would affect the ratio observed in any gas reservoir, however. The age and composition of the rocks contributing gases would be most important and other contributing factors would be the porosity of the reservoir and the total pressure. Since helium would be expected to diffuse through silicates more readily than the other inert gases, it would be lost from a reservoir more easily than argon. It is reasonable, then, to expect to observe a helium-to-argon ratio lower than theoretical in most natural sources. As a result, very little can be concluded from natural gas sources, except that a helium-to-argon ratio of less than 2.8 indicates that either the source of the gas had higher uranium and thorium to potassium ratio than average rocks or that helium has been depleted in the reservoir. A low ratio cannot indicate a source of an age much greater than the presently accepted age of the earth.

If the inherited argon and helium found in inclusions is assumed to have originated as magmatic gas, then the argon and helium released from these rocks could be representative of the magmatic gases. Table IV presents the helium-to-argon ratios found in this study. The ratios are generally less than one and all but five are less than two. Of the remaining five only one, HK-173, can be considered, with any certainty, to have a high helium-to-argon ratio. In the other cases the small amount of one or the other gas

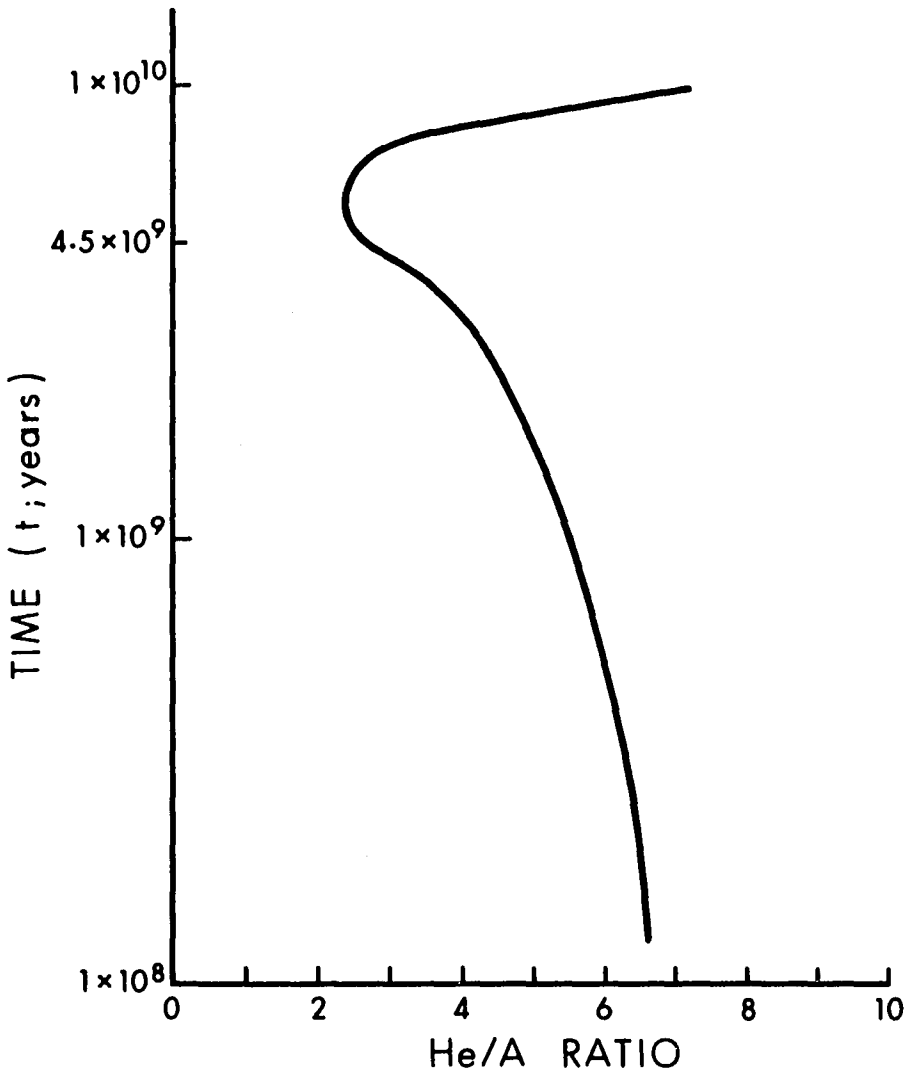

Figure 8

Helium-to-Argon Ratio as a Function of Time

makes the ratio uncertain. A relatively large amount of helium was found in the deep ocean tholeiite sample HK-173 and although a large uncertainty (> 100%) in the argon measurement makes it difficult to assign an exact helium-to-argon ratio, the ratio is probably higher than found for the other rocks and minerals.

The uranium, thorium and potassium analyses from this work and other sources[43,58] indicate that the ratios of the concentrations of these elements in olivine nodules are similar to those postulated for an average rock by Zartman et al. If the inert gases found in the inclusions originated from the respective radioactive elements in the rock, then the minimum ratio that could be found (see Figure 8) would be approximately 2.8 unless the helium and argon diffuse out of the mineral at different rates. Amirkanoff did not find this to be the case for pyroxene at 900°C.[4] However, there is a possibility of more than one mode of diffusion. Amirkanoff considered his data to represent lattice diffusion. Different rates would be expected for diffusion along grain boundaries and microcracks or from trapping sites. Since these parameters can be expected to vary greatly from sample to sample as a result of different thermal histories and are also very difficult to describe quantitatively, it can be seen that very little quantitative information could be gained through examination of helium-to-argon ratios unless much more is known about diffusion processes than is presently the case.

E. Location of Gases in Inclusions.

This attempt to investigate the rare gas content of the ultramafic inclusions was undertaken because of the anomalous old ages found for some of these and because of the possibility that some information might be gained that could be applied to the investigation of magmatic gases. The size and availability of the inclusions from the 1801 Kaupulehu flow of Hualalai, Hawaii, was an added inducement. The first nodule investigated was specimen HK-160. Figure 9 presents the argon contents of the sections of this nodule found by fusion and by crushing. A definite concentration gradient exists for argon and for helium, although less data is available for the latter (see Table IV). The existence of this gradient suggested that it might be possible to find a nodule large enough, or one that had been in a high temperature environment for such a short time, that little gas would have escaped from the center of the nodule. However, the next nodules investigated (HK-161, HK-167, and HK-166) did not reveal such a region. Moreover, in the case of feldspar HK-167, the outer section had a higher argon content than the center section. A reasonable explanation for this is that the nodules as found on the surface of the earth may be fragments of larger nodules and they may or may not have had time to come to a quasi-equilibrium state in regard to the rare gas distribution in the nodule. Further support of this proposal can be found in the

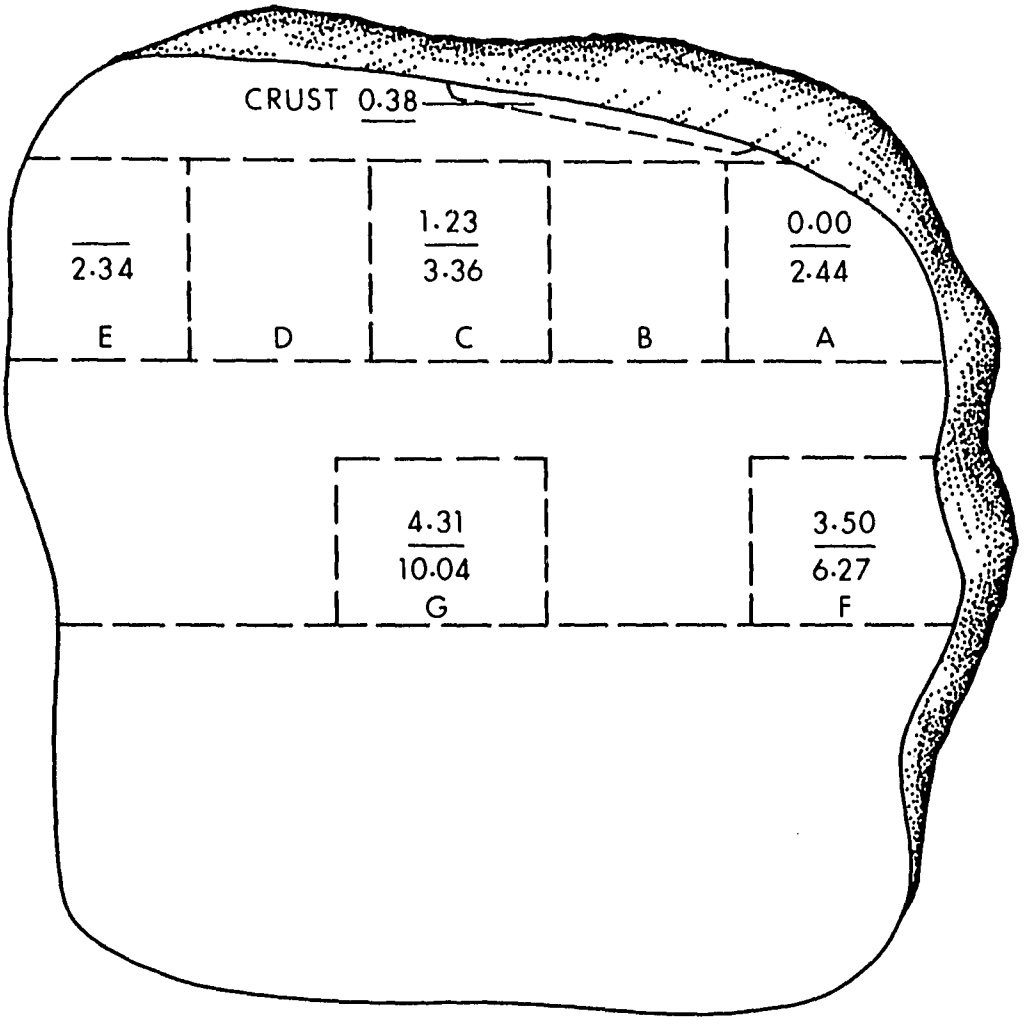

All values listed are std. $cm^3 \times 10^7$/gm, upper values obtained by crushing technique lower values obtained by fusion technique.

Figure 9

Radiogenic Argon Content of Sections of a Nodule (HK-160) from the 1801 Kaupulehu Flow, Hualalai

observation that almost all the inclusions found at Hualalai have one or more flat sides. This suggests fracture from a larger rock rather than formation by the gradual accumulation of small crystallites which would probably result in a generally spherical shape. As a result, the probability of finding a nodule with a relatively un-degassed section becomes a matter of chance rather than size.

The fact that the gradients do exist indicates that diffusion losses have taken place. This is not surprising in view of the probable temperature of the magma ($\sim$1100°C) and the diffusion coefficient measured by Amirkanoff.[4] This diffusion constant makes it seem unlikely, in fact, that any argon or helium would be found in these inclusions at all. This, in turn, leads to the speculation that the argon and helium may have been forced into microcracks and trapped by closure and annealing of the cracks at a later date. It is also possible that a relatively high pressure of the gases exists at great depths and the gases represent an equilibrium concentration dissolved in the mineral that would vary with mineral type and with the position of the inclusion in the magma chamber.

If the value found by Amirkanoff for the diffusion coefficient of argon in pyroxene is assumed to be applicable to olivine and is also assumed to be due to volume diffusion, then the only condition that would result in the argon and helium being retained for any length of time would be

inclusion of the gas in a fluid inclusion. The action of such holes as traps which slow down over-all diffusion rates in solids, even at very high temperatures, is known from studies of fission gas escape from ceramic fuel elements in atomic reactors.[46] If this trapping mechanism is effective here, the over-all diffusion coefficient for the included inert gases would probably be substantially lower[20,46] than expected since there would be a potential barrier at the fluid-crystal interface. This is a possible explanation for the presence of the argon and helium. More substantial proof of the location of the helium and argon in the fluid inclusions is the fact that crushing releases inert gases. If the gases were located in the lattice, very little argon should be lost upon grinding most minerals. This has also been demonstrated by Funkhouser, Naughton, and Barnes.[23]

F. Origin of the Inclusions.

The origin of the inclusions such as dunites and eclogites has been a subject of controversy for some time.[24,56,61] Much of the speculation has revolved around deciding which of these inclusions are xenolithic in respect to the formations in which they are found and which, if any, are representative of the mantle. It was thought that an investigation of the inert gas content of these inclusions might shed some light in these areas. The inclusions could have crystallized relatively recently in the magma or they

could be fragments of the mantle. With reference to the latter, White[61] has pointed out that the mantle fragments might or might not be representative of the primary mantle material since it is not known whether the mantle is homogeneous or whether the fragments are the insoluble residue from a fusion of mantle material. Obviously, since more than one origin can be reasonable postulated it is possible that some inclusions have one source and other inclusions a different source. Inclusions from four different locations were investigated in this study: (1) Hualalai, Hawaii; (2) Salt Lake, Oahu; (3) East Kilauea rift zone, Hawaii; and (4) Bultfontein, Republic of South Africa. The South African sample was included to provide comparison with a specimen from a location geographically removed from the Hawaiian samples. The three Hawaiian locations are representative of three types of basaltic hosts: (1) olivine nephelinite (Salt Lake); (2) alkaline olivine basalt (Hualalai); and (3) olivine tholeiite (east rift zone of Kilauea).

White[61] has discussed Hawaiian inclusions at length and finds, on the basis of petrographic and electron microprobe studies that the basaltic hosts and their inclusions are separable into three distinct suites, represented by the above specimens. His conclusions are (1) the tholeiitic olivine inclusions were crystallized from the host magma; (2) the alkaline olivine inclusions are accumulates of

crystals from the baltic magma, and (3) the lherzolite inclusions in olivine nephelinite probably had their origin in the mantle.

Examination of the data in Tables III and IV for the specimens from these four locations will show that the differences in total helium content, total argon content or in helium to argon that exist between inclusions of different geographic origin is no greater than those found within the inclusions from one location. The two possible exceptions to this are the very low argon content found for the Salt Lake sample and the unusually high helium content found for the Bultfontein olivine and pyroxene. Since Funkhouser [22] did find excess argon in a similar Salt Lake olivine it is possible that the specimens chosen for this study were not typical of the olivines in this area. Holmes and Paneth[31] have reported studies involving minerals from the Bultfontein area that have a high uranium content (~1 ppm) and they have also pointed out that minor amounts of zircon can be found in some of these inclusions. Either of these two possibilities could explain the greater helium content of these minerals in comparison to the other inclusions investigated in this study.

As has been pointed out previously, the absolute inert gas contents vary widely from one sample to another. However, the fact that the helium-to-argon ratios from each source are fairly consistent suggests that one mechanism

exists for the incorporation of inert gases into the inclusion. The most likely mechanism is one involving entry of the gases into the mineral, either by diffusion into traps or by physical entrapment through annealing of microcracks, while in the magma environment. Whether the inclusion was a segregative fragment or a fragment of the mantle or a conduit wall would make little difference if the time spent in the magma was long compared to the time needed for a quasi-equilibrium state to become established.

As a result, the data presented in this study offers little assistance to those who would unequivocably assign different origins to the inclusions found in the three types of basaltic hosts mentioned above. It is possible, however, that if a great number of carefully chosen samples from each location were analyzed that a real difference might appear.

G. Origin of the Inert Gas.

The origin of the inert gases found in the ultramafic inclusions has actually been discussed in earlier sections in relation to other aspects of this study so this section will serve mainly to summarize these arguments.

Since the diffusion coefficient of argon and helium in pyroxene is so high, it is reasonable to assume that very little of the inert gas content of these inclusions is of internal radiogenic origin. Further support of this proposal is found in the release of the inert gas by crushing.

However, the possibility that the inert gases were generated in inclusions from trapped potassium or uranium still existed so an attempt was made to determine whether or not a concentration gradient for potassium similar to that found for argon existed. The analyses presented in Table V are not very precise, but they show it is unlikely that the same gradient exists for potassium as does for argon. The ratio of the argon contents for the center to edge sections in HK-160 (Table III) was 3 and the ratio for the potassium analysis of the same sections was 0.5. The high potassium level for HK-160-E was probably due to the small amount of basaltic crust on the outer edge of this sample. In the other case, HK-166, the ratios were similar, 0.57 and 0.63. These results are rather inconclusive in that it is still possible that similar gradients existed prior to loss of the inert gases by diffusion. In either case, ages could not be calculated from the results with any degree of certainty.

The inert gases found in the deep ocean tholeiites are almost certainly of magmatic origin, since as stated previously, the samples are probably less than 200 years old. The conditions of extrusion for submarine magma, that is, high pressure and rapid cooling, would result in much less degassing of the solidifying basalt than if the lava had been extruded subaerially. As a result it seems reasonable to assume that these samples contain inert gases that are

representative of those found in the magma environment just prior to eruption. That some degassing may have taken place is suggested by the fact that the absolute amount of argon found in the three samples varies directly with the sampling depth. It is possible, however, that this variation is not due to the effect of varying pressure on the amount of degassing but is the result of an actual variation in the argon content of the magma with depth. If the variation of argon content with depth was the result of degassing one would expect the helium contents to be affected even more severely, since helium is lighter than argon. However, the opposite effect is observed. The sample from the shallowest eruption is the only one that contained a significant amount of helium. This data is presented in Figure 10. Moore[49] has reported that the amount of olivine in these samples increases with depth and so this might be offered as an explanation for the variation of argon observed. However, the argon content of the separated olivine (Table III) was not high enough to account for all the argon found in the whole rock. If allowance is made for the small amount of plagioclase and pyroxene present the argon estimated as being present in the inclusions is still only 50% of the total. The presence of a significant amount of inert gas in the glassy part of the tholeiite is further supported by the presence of argon in the crushed sample.

If the assumption is then made that most of the whole rock inert gas is trapped in the basalt rather than the inclusions, then the gas must be magmatic in origin. If this is the case then one is forced to the conclusion that the magma extruding from the 1400 meter level contained more helium than that at the lower levels. There are at least two possible causes. The first is that the magma extruded from the shallower depth had dissolved a local deposit of helium-bearing minerals (i.e., zircon or beryl). This seems very unlikely in that a very large deposit would have to dissolve to release a significant amount of gas and that one would expect to find fragments of these minerals in the basalt. Another possibility is that gaseous differentiation occurs in the magma with the lighter helium being concentrated in lower pressure areas. If this is the case, then with proper sampling, it may be possible to establish a relation between inert gas content and the depth of the magma reservoir.

The helium-to-argon ratios found for the deepest basaltic samples are similar to those found for the inclusions, that is, they are less than that predicted for an average rock. The shallowest basaltic sample had a helium-to-argon ratio greater than expected for an average rock, however, and since these extrusions were probably fed from a single summit reservoir, one must conclude that some diffusion or distillation mechanism is altering the helium-to-argon ratio of the dissolved gases. This occurrence would limit the

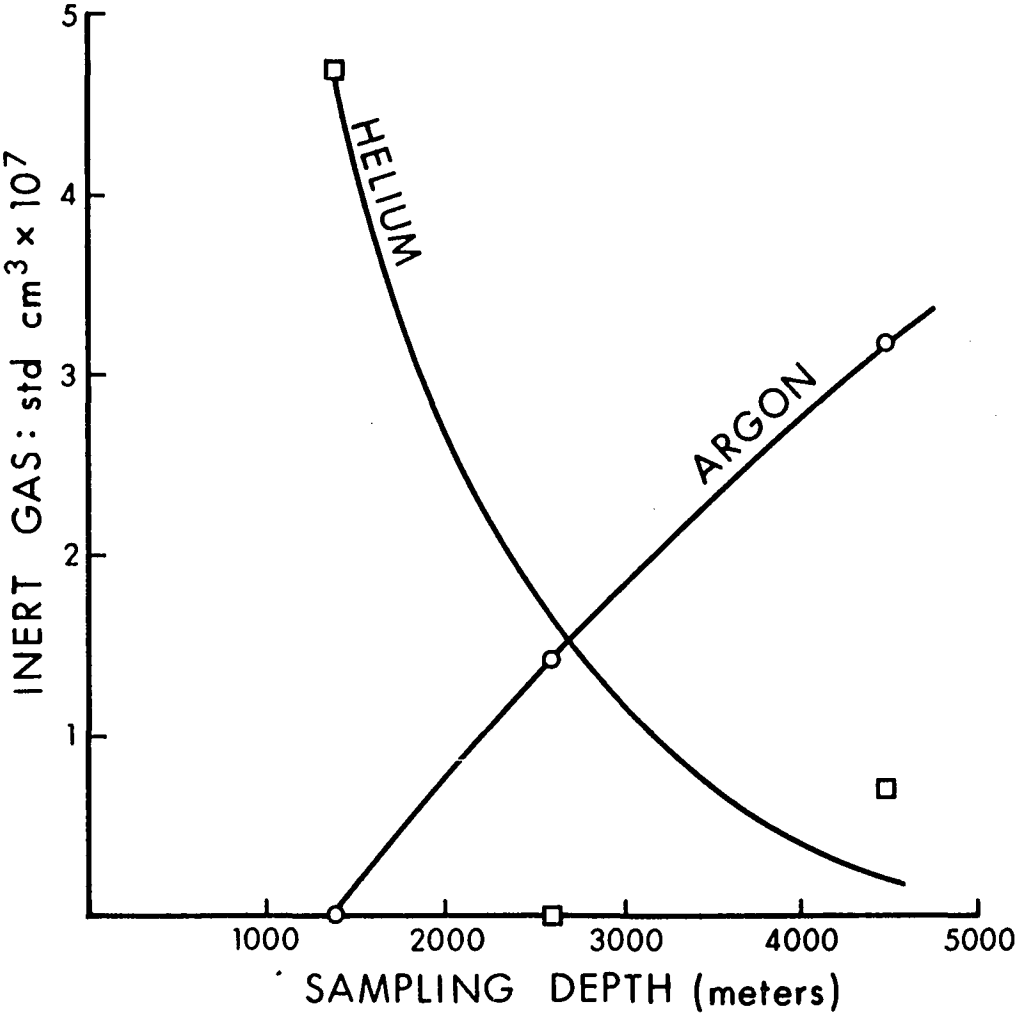

Figure 10

Inert Gas Content of Deep Ocean Tholeiite Samples
as a Function of Sampling Depth

uses of the included inert gas ratio as an indicator of the age of magma or of any accumulates from the magma.

In the course of this study an attempt was made to ascertain whether the argon content of the olivine in a nodule was affected by alteration of the olivine to iddingsite. It had previously been reported[22] that no loss in argon occurred as a result of alteration of olivine to iddingsite. The work reported here shows an appreciable loss (Table III, HK-168) and definitely does not support this view.

IV. Summary

A. Suggestions for Equipment Improvement

It has been pointed out at several points in the foregoing discussion that equipment limitations have restricted the research being reported in this study. It would be desirable, for the guidance of future workers at this laboratory, to summarize these limitations and make specific suggestions for improvement.

In order to elucidate the mechanism for the processes taking place in geologic systems there is needed further and more precise diffusion studies in silicate systems. It is believed that the analytical measurements for such studies would be best made by mass spectrometry. However, solution of the equations describing diffusion from irregular spherical particles usually set a limitation of one percent of the total gas for the measured amount of diffused gas. The amount of inert gas found in most inclusions is much too small for one to detect accurately one percent of the inert gas with the existing equipment. Using larger samples would call for much larger gettering capacity than is presently available. A much more satisfactory solution would be to replace the Faraday cage ion detector on the mass spectrometer that is now in use, with an electron-multiplier detector. It would also be desirable to provide a separate electrical system for focusing the helium peak. A switching arrangement would then make determination of the argon and

helium peak heights more rapid and probably increase the sensitivity of the instrument for helium. Another improvement in the helium determination could be achieved by constructing most of the extraction and tracer system of high alumina glass (i.e. Corning 1720) to reduce helium diffusion into the vacuum system.

The other step that must be taken to widen research on inclusions is to develop a rapid and sensitive method for potassium analysis of ultramafic minerals. It is felt that the solid state mass spectrometer constructed at this laboratory[63] merits more effort in this direction. It is possible that a more sophisticated filament current regulator or perhaps indirect sample heating could eliminate the instability that has been encountered using this instrument.

Another area of improvement involves the time and effort involved in each gas extraction and determination. Since the amount of inert gases found in these inclusions is small and variable, replicate determinations are usually desirable. Even though the time and effort needed for each determination was greatly reduced during the course of this study, the operation of the extraction equipment still requires a great deal of attention. Addition of timing devices would obviate much of the busy work connected with each determination.

B. Suggestions for Future Work

It is felt that future work should follow three main courses:

1. Solid state diffusion studies on silicates patterned after those of MacEwen and Stevens[46] on uranium dioxide.

2. An increased number of determinations of the specific inclusions studied herein to verify the present results and more accurately ascertain the inert gas content of these inclusions.

3. An investigation of inclusions containing "excess" argon that are not of a suspected mantle origin, i.e., the biotites from Salt Lake, Oahu. Further work may ascertain whether or not the ages found for these minerals are consistent or are the result of random minor inclusion of argon from the magma environment.

C. Conclusions

The result of this study may be summarized as follows:

1. The inert gas found in the ultramafic inclusions studied is probably located in fluid inclusions. The possibility of the gas being held in trapping sites should not be completely ruled out, as it is felt that careful diffusion studies would be needed to decide between the two possible mechanisms for trapping gas in a crystalline material. The best evidence in favor of the location of the gas in the fluid inclusions is the release of a large part of the gas by crushing.

2. The inert gas in these ultramafic inclusions is probably magmatic in origin. In support of this view is the similarity of the helium-to-argon ratios found for inclusions from different sources and the similarity of the helium-to-argon ratios found for the inclusions to that found for an apparent magmatic source, the deep ocean tholeiite. The high diffusion coefficient for argon in pyroxene would preclude long time argon retention by minerals at high temperatures in an argon-poor environment.

3. Meaningful and unequivocal age determinations cannot be made at the present time using the helium and argon contents of these inclusions.

4. Deep ocean basalts from greater than 1400 meters are probably not suitable for age dating.

5. The alteration of olivine to iddingsite and probably other mineral alterations results in loss of radiogenic argon.

6. Improvements in technique for the extraction and determination of argon and helium in ultramafic inclusions have been worked out but more are needed to enable the volume of work required for a detailed study to be accomplished.

Bibliography

1) Aherns, L. H., Nature, 157, 269 (1946).

2) Aldrich, L. T., and Nier, A. O., Phys. Rev., 74, 876 (1948).

3) Aldrich, L. T., and Wetherill, G. W., Ann. Rev. Nucl. Sci. 8, 257 (1958).

4) Amirkhanoff, K. I., Brandt, S. B., and Barnitsky, E. N., Ann. N. Y. Acad. Sci., 91, 235 (1961).

5) Armstrong, R. L., in "Potassium Argon Dating" compiled by Schaffer, O. A. and Zahringer, J., Springer-Verlag New York Inc., (1966) p 119.

6) Barrell, J., Geol. Soc. Am. Bull., 28, 745 (1917).

7) Biondi, M. A., Rev. Sci. Instr., 30, 831 (1959).

8) Boltwood, B. B., Am. J. Sci., 23, 77 (1907).

9) Brookin, D. G., and Hurley, P. M., Am. J. Sci., 263, 1 (1965).

10) Cuvier, G. and Brongniart, P., J. Mines XXII, 421 (1808).

11) Dalrymple, G. B. and Lanphere, M. A., Nature, 209, 902 (1966).

12) Damon, P. E. and Kulp, J. L., Trans. Am. Geophy. Union, 38, 945 (1957).

13) Dean, J. A. in "Instrumental Methods of Analysis" 3rd ed. by Willard, H. H., Merritt, L. L., and Dean, J. A., Van Nostrand, Princeton, New Jersey, (1958) p 248.

14) Dushman, S., "Scientific Foundations of Vacuum Technique" John Wiley and Sons., New York (1962).

15) Elliot, R. M., in "Mass Spectrometry" McDowell, C. A., Ed., McGraw Hill, New York, (1963) p 75.

16) Endt, P. M. and Kluyver, J. C., Rev. Mod. Phys., 26, 96 (1954).

17) Evernden, J. F., Savage, D. E., Curtis, G. H., and Jones, G. T., Am. J. Sci., 262, 145 (1964).

18) Fairbairn, H. W. and Hurley, P. M., Trans. Am. Geophys. Union, 38, 99 (1957).

19) Faul, H., in "Nuclear Geology", Faul, H. Ed., John Wiley and Sons, New York, (1954) p 256.

20) Fechtig, H. and Kalbitzer, S., in "Potassium Argon Dating" compiled by Schaffer, O. A. and Zahringer, J., Springer-Verlag New York Inc., (1966) p 74.

21) Fleisher, R. L. and Price, P. B., Geochim, Cosmochim. Acta., 28, 1705 (1964).

22) Funkhouser, J. G., Ph.D. Dissertation, Univ. of Hawaii, Jan., 1966.

23) Funkhouser, J. G. Barnes, I. L., and Naughton, J. J., Bull. Volcanologique, XXIX, 709 (1966).

24) Green, D. H., Earth and Planetary Sci. Letters, 1, 414 (1966).

25) Gubelin, E. J., "Inclusions as a Means of Gemstone Identification" Am. Soc. of Gemologists, Los Angeles, 19.

26) Hamilton, E. I., "Applied Geochronology", Academic Press, N. Y. (1965).

27) Herr, W. and Merz, E., in "Radioisotopes in Scientific Research", Vol. II, Ed. Extermann, R. C., Pergamon Press, London, (1958) p 571.

28) Heymann, D. and Keur, E., J. Sci. Instr., 42, 121 (1965).

29) Hirt, B., Herr, W. and Hoffmeister, W. in "Radioactive Dating" I.A.E.A., Vienna, (1963) p 35.

30) Holland, H. D., in "Nuclear Geology" Faul, H. Ed., John Wiley and Sons, (1954) p 175.

31) Holmes, A. and Paneth, F., Proc. Roy. Soc., 154, 385 (1936).

32) Houterman, H. G. in "Potassium Argon Dating", compiled by Schaffer, O. A. and Zahringer, J., Springer-Verlag, New York (1966) p 1.

33) Hurley, P. M., Trans. Am. Geophys. Union, 33, 174 (1952).

34) Hurley, P. M. in "Nuclear Geology" Faul, H. Ed., John Wiley and Sons (1954) p 301.

35) Hurst, D. G., Atom. Energy Can. Report AECL- 1550 (1962).

36) Jackson, E. D., Geol. Soc. Ame., Abstracts Annual Meeting (1966).

37) Kirsten, T., in "Potassium Argon Dating" compiled by Schaffer, O. A. and Zahringer, J., Springer-Verlag, New York (1966) p 19.

38) Lanphere, M. A. and Dalrymple, G. B., J. Geophys. Res., 70, 3497 (1965).

39) Libby, W. F., Phys. Rev., 69, 671 (1946).

40) Lipson, J., Geol. Soc. Am. Bull., 69, 137 (1958).

41) Livingston, R., "Physico Chemical Experiments", MacMillan Co., N. Y. (1947).

42) Lovering, J. F. and Morgan, J. W., Nature, 197, 138 (1963).

43) Lovering, J. F. and Morgan, J. W., Nature, 199, 479 (1963).

44) Lovering, J. F. and Richards, J. R., J. Geophys. Res., 69, 4895 (1964).

45) Lyell, C., "Elements of Geology", J. Murry, London (1841).

46) MacEwan, J. R. and Stevens, W. H., J. Nuclear Materials, 11, 77 (1964).

47) McDougall, I., Geol. Soc. Am. Bull., 75, 107 (1964).

48) Moberly, R. M., Univ. of Hawaii, Personal Communication, Dec. 1967.

49) Moore, J. G., Am. J. Sci., 263, 40 (1965).

50) Muller, O. in "Potassium Argon Dating", compiled by Schaffer, O. A. and Zahringer, J., Springer-Verlag, New York, (1966) p 40.

51) Nier, A., Phys. Rev. 60, 112 (1947).

52) Price, P. B. and Walker, R. M., J. Geophys. Res., 68, 4847 (1963).

53) Rankama, K., "Progress in Isotope Geology", Wiley, New York (1963).

54) Reynolds, J. H., Rev. Sci. Instr., 27, 928 (1956).

55) Roedder, E., Am. Miner., 50, 1746 (1965).

56) Ross, C. S., Foster, M. D., and Myers, A. T., Am. Miner., 39, 693 (1954).

57) Stearns, H. S., "Geology of the State of Hawaii", Pacific Books, (1966) p 75.

58) Tilton, G. R. andReed, G. W., in "Earth Science and Meteoritics" compiled by Geiss, and Goldberg, (1963) p 31.

59) Volchok, H. L. and Kulp, J. L., Geochim. et. Cosmochim. Acta. 11, 219 (1957).

60) Wasserburg, G. J., in "Nuclear Geology", Faul, H. Ed., John Wiley and Sons, New York, (1954), p 341.

61) White, R. W., Contr. Mineral. and Petrol., 12, 245 (1966).

62) Winchell, H., Geol. Soc. Am. Bull., 58, 1 (1947).

63) Yamashiro, C. H., M. S. Dissertation, Univ. of Hawaii, Chem. Dept. (1965).

64) Zartman, R. E., Wasserburg, G. J., and Reynolds, J. H., J. Geophys. Res., 66, 277 (1961).